Journal of Zoological Systematics and Evolutionary Research

WILEY

Research Article

Open Access

https://doi.org/10.48130/jzser-0026-0002

Journal of Zoological Systematics and Evolutionary Research **2026**, 2026: e003

Integrative taxonomy of *Spauligodon* (Nematoda: Oxyurida: Pharyngodonidae) with the description of two new species from desert lizards in Turpan Basin, China

Xiaofei Yan[1,2*#], Ziqi Jiang[1,2#], Yi Ba[1,2], Chong Liu[1,2], Shengtao Chen[1,2], Tao Wang[1,2], Yiyang Zhao[3], and Shuxian Li[1,2]

[1] *Xinjiang Key Laboratory for Ecological Adaptation and Evolution of Extreme Environment Organisms, Xinjiang Agricultural University, Urumqi, Xinjiang Uygur Autonomous Region 830052, China*

[2] *College of Life Sciences, Xinjiang Agricultural University, Urumqi, Xinjiang Uygur Autonomous Region 830052, China*

[3] *College of Veterinary Medicine, Xinjiang Agricultural University, Urumqi, Xinjiang Uygur Autonomous Region 830052, China*

[#] Authors contributed equally: Xiaofei Yan, Ziqi Jiang

[*] Correspondence: yanxf83@163.com or 120220031@xjau.edu.cn (Yan X)

Abstract

Spauligodon is a genus of parasitic nematodes that inhabit the intestinal tracts of lizards, with infections occurring frequently in carnivorous and omnivorous hosts. Although over 50 species have been described, the accurate delimitation of new species and confirmation of the taxonomic stability of previously described taxa have been impeded by ambiguous diagnostic characteristics; this issue is often compounded by male dimorphism and a limited number of phylogenetic analyses. *Eremias roborowskii* and *Teratoscincus roborowskii* are two omnivorous desert lizards endemic to the Turpan Basin of Xinjiang, China. In this study, we employed an integrative taxonomic framework combining comparative morphology and multi-locus phylogenetic analyses (*18S* + *28S* + *COI*, along with mitochondrial *COI*). We identified two new species of *Spauligodon* isolated from the intestines of these two lizard hosts, and, using newly defined morphological diagnostic characters, we constructed a dichotomous identification key for the genus. The two nematode species are herein designated *Spauligodon turpanoeremius* sp. nov. and *S. turpanoscincus* sp. nov. Phylogenetic analyses utilizing Bayesian Inference and Maximum Likelihood trees, based on concatenated multi-locus and mitochondrial *COI* datasets, revealed high topological congruence. The two new species formed distinct, well-supported evolutionary clades that clustered separately from other congeners, thereby clarifying the phylogenetic placement of the taxa. By adopting this integrative taxonomic approach, we not only describe two new species of *Spauligodon* from the Palaearctic realm but also further refine the taxonomic identification system for the genus. This approach substantially alleviates the confounding effects of male dimorphism and enhances the reliability of morphological identification. Furthermore, our findings provide key morphological and molecular evidence for further elucidating host-driven evolutionary mechanisms in host–parasite associations and the role of host diet in shaping parasitic adaptation.

Keywords: Desert lizards, *Spauligodon*, Integrated taxonomy, Male dimorphism, Molecular phylogenetics, Diet

Citation: Yan X, Jiang Z, Ba Y, Liu C, Chen S, et al. 2026. Integrative taxonomy of *Spauligodon* (Nematoda: Oxyurida: Pharyngodonidae) with the description of two new species from desert lizards in Turpan Basin, China. *Journal of Zoological Systematics and Evolutionary Research* 2026: e003 https://doi.org/10.48130/jzser-0026-0002

Introduction

The family Pharyngodonidae (Nematoda: Oxyurida) comprises 24 genera, including parasites that infect fish, amphibians, reptiles, and mammals[1–3]. The genus *Spauligodon* Skrjabin, Schikhobalova, and Lagodovskaja 1960 encompasses 57 recognized species that predominantly inhabit the intestinal tracts of reptilian hosts[4–8]. These parasites are particularly prevalent in carnivorous and omnivorous lizards[9], with frequent occurrences documented among members of the families Gekkonidae, Lacertidae, and Scincidae[10]. Nematodes in this genus are known to be globally distributed, with records spanning Asia, Africa, North America, South America, Europe, and Oceania[11,12]. However, to date, reports from China remain extremely limited; only Wang et al.[13] and Yan et al.[14] have conducted preliminary surveys examining *Spauligodon* infections in desert-dwelling lizards from Xinjiang, China.

Given the high similarity of the females among different taxa within the family Pharyngodonidae, taxonomic identification is largely dependent on male morphological characteristics[2,15]. This morphological stasis is further compounded by convergent evolution, whereby similar selective pressures promote correspondingly similar evolutionary adaptations in distantly related species, resulting in limited morphological divergence among closely related parasitic species[16]. Consequently, species delineation based solely on morphological traits can prove challenging[17,18]. For instance, species of the genus *Spauligodon* have several key diagnostic features in common with those of the genus *Skrjabinodon*[19,20], and the species of both are often characterized by male dimorphism[21,22]. The presence or absence of caudal alae has, nevertheless, been established to be a key distinguishing trait[21,23]. Historically, many morphological approaches have designated *Spauligodon* species based solely on male morphology, often overlooking male dimorphism and other diagnostic discrepancies; this has led to potential misclassification as *Skrjabinodon*[21]. Similar issues of morphological overlap can occur randomly among other genera within Pharyngodonidae[24]. Consequently, the inconsistent application of diagnostic criteria within *Spauligodon*, the prevalence of overlapping morphological traits, and subtle interspecific differentiation collectively undermine the reliability of species identification within this genus[5,11,25].

https://doi.org/10.48130/jzser-0026-0002

The Turpan Basin in the Xinjiang Uygur Autonomous Region of China has a typical continental arid climate. Extreme environmental conditions in this region—including scant rainfall, low humidity, and intense evaporation[26]—have contributed to the evolution of *Teratoscincus roborowskii* and *Eremias roborowskii,* two endemic species of omnivorous desert lizards. The former feeds primarily on small arthropods and the plant *Capparis spinosa*[27,28], the fruit of which also constitutes a significant proportion of the latter's diet[29]. Both species facilitate the germination of *Capparis spinosa* seeds, and serve as important ecological seed dispersers[30]. Seed dispersal represents a crucial component of plant–animal interactions[31,32], the effectiveness of which is profoundly influenced by the interaction between seeds and the animal digestive tract[33]. However, oxyurids do not feed on host tissue but instead consume bacteria in the hindgut or cecum. Therefore, the effect on host health is generally low, with little to no pathogenicity[34]. Nevertheless, they may alter the microbial environment within the lizard's digestive tract that is conducive to seed germination, thereby affecting seed dispersal. The direct life history of oxyurids is fairly similar across the groups that parasitize vertebrates and invertebrates[35,36]: the genus *Spauligodon* may utilize arthropods that feed on decaying plant material as transport hosts; Oxyurids have no free-living or extraintestinal stages, and following ingestion of the arthropod by a carnivorous or omnivorous lizard, the larvae hatch directly from eggs within the new host and subsequently remain in the intestinal tract for their entire life cycle[37,38], meaning that they can have a highly aggregated distribution within host species[39]. Although *Eremias roborowskii* and *Teratoscincus roborowskii* feed on both plant seeds and insects, the proportions of these two components in the diets of these lizards undergo seasonal fluctuations[27,28]. These dietary shifts influence the intensity of nematode infections within the host, ultimately modifying alterations in the structure of the parasite community. Consequently, pharyngodonid nematodes that parasitize the intestinal tract represent a significant factor influencing the health and population dynamics of these desert lizards, as well as the effective dispersal of seeds among local *Capparis spinosa* populations.

To address the prevailing taxonomic challenges within the genus *Spauligodon*, this research employed an integrative approach combining comparative morphology with phylogenetic analysis based on nuclear *18S* rRNA, *28S* rRNA, and mitochondrial cytochrome *c* oxidase subunit I (*COI*) gene regions. Based on these findings, we undertook a revision of the diagnostic characteristics of the genus and constructed a dichotomous identification key. Consequently, we identified two new species of *Spauligodon* as intestinal parasites of *Eremias roborowskii* and *Teratoscincus roborowskii* inhabiting the Turpan Basin. We thus believe that this research will make a significant contribution to the clarification of the phylogenetic affiliations of *Spauligodon* within the family Pharyngodonidae, as well as augmenting the known diversity of helminth parasites in Chinese desert lizards.

Materials and methods

Parasite collection

During the 2024–2025 field seasons, a total of 36 *Eremias roborowskii* and 9 *Teratoscincus roborowskii* individuals were randomly sampled from the Turpan Basin in Xinjiang Uygur Autonomous Region, China (Figs 1, 2). Of the total specimens, an additional 20 individuals each of *Eremias roborowskii* and *Teratoscincus roborowskii* were obtained from the permanent specimen collection preserved long-term in 4% formalin (deposited in the Specimen Repository of Xinjiang Agricultural University). Following euthanasia via intraperitoneal injection of sodium pentobarbital, the digestive tract was examined under a stereomicroscope. The esophagus, stomach, small intestine, and large intestine were systematically dissected and examined. Collected nematode specimens were rinsed with physiological saline to remove adhering debris and subsequently preserved in a glycerol–ethanol conservation medium (5% glycerol, 80% ethanol). All specimens were deposited in accordance with international biobanking standards at the National Parasite Resource Center of China and assigned accession numbers (Registration ID: 24F00015BQN~24F0001aS6D, 60 specimens). Illustrations and maps were prepared and constructed using Adobe Illustrator 28.0 and ArcGIS Pro 3.5.2 software, respectively.

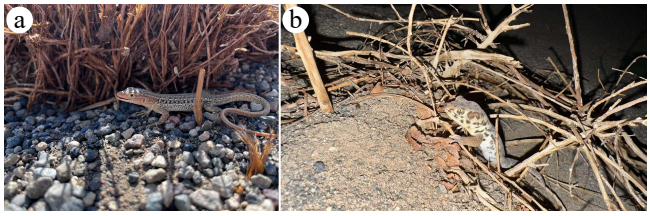

Fig. 1 Wild foraging habitats of the two lizard species in the Turpan Basin, Xinjiang Uygur Autonomous Region, China. (a) *Eremias roborowskii* inhabiting an area beneath *Alhagi camelorum* in the wild. (b) *Teratoscincus roborowskii* crawling in the wild.

Morphological observation

Nematodes were cleared in lactophenol and examined using a digital microscope (Motic BA210) integrated with a microscopic image acquisition and analysis system. For scanning electron microscopy (SEM) observation, specimens were sequentially rinsed in 0.2 mol/L phosphate buffer (PB) and fixed overnight in FAA (formaldehyde–acetic acid–ethanol–glycerol standard fixative). Following an additional PB rinse, the specimens were fixed again in FAA for 2 h. After further PB rinsing, dehydration was carried out through a graded ethanol series (50%–100%), each step lasting 15 min. The specimens were then subjected to tert-butanol substitution, freeze-dried, and gold sputter-coated. The observations and imaging were performed using a Zeiss Supra 55 VP SEM at an accelerating voltage of 2 kV[14]. The prevalence and intensity of nematode infections were calculated according to Yan et al.[40]. A dichotomous identification key for the genus was constructed based on the differential morphological characteristics among species. All measurements are provided in micrometers (μm), unless otherwise indicated.

Molecular procedures

Genomic DNA was extracted from nematode specimens using the Tiangen Micro DNA Extraction Kit (Tiangen Biotech, Beijing, China). The nuclear *18S* rRNA, *28S* rRNA, and mitochondrial *COI* gene were subsequently amplified via polymerase chain reaction (Table 1). The primer information and cycling conditions for amplifying the different target regions are provided in Supplementary Table S1. After post-electrophoresis quality assessment using GoldView™-stained agarose gels (1.5%), amplified DNA fragments underwent commercial purification (Sangon Biotech, Shanghai, China) followed by bidirectional Sanger sequencing on an ABI PRISM® 3730 platform (Applied Biosystems) to ensure sequence fidelity. Raw sequences were assembled using DNAMAN 9.0, with manual correction, followed by BLAST searches against the National Center for Biotechnology Information (NCBI) database (https://blast.ncbi.nlm.nih.gov)[13]. The *18S*, *28S*, and *COI* sequence data generated in this study have been deposited into the GenBank database (www.ncbi.nlm.nih.gov).

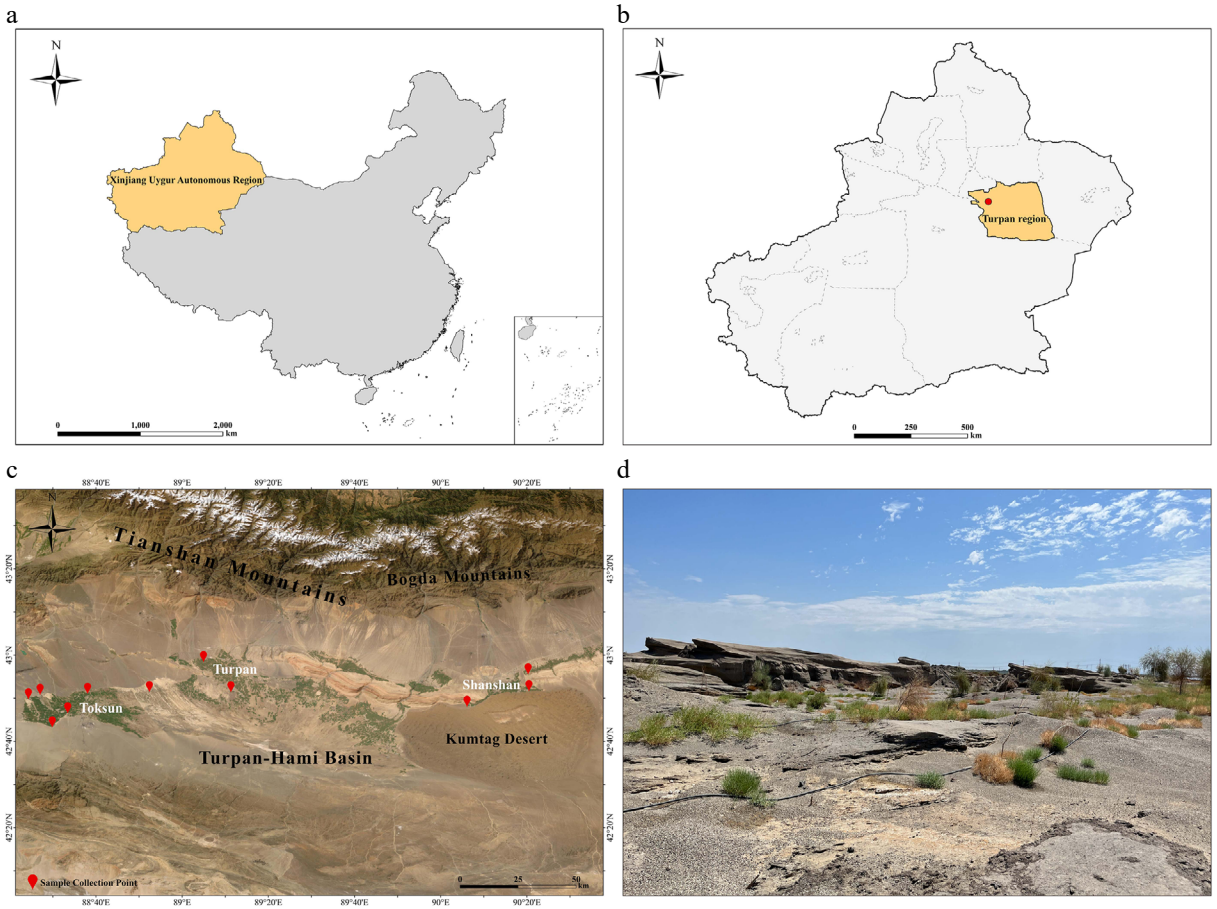

Fig. 2 Sampling sites and geographic distribution of the two lizard species collected during 2024–2025 field surveys in the Turpan Basin, Xinjiang, China. (a) Map of the People's Republic of China, highlighting the location of the Xinjiang Uygur Autonomous Region. (b) Map of the Xinjiang Uygur Autonomous Region, indicating the Turpan research area. (c) Topographic map of the Turpan Basin, with red markers denoting sampling sites in Toksun, Turpan, and Shanshan. (d) Representative arid desert habitat of the research region, illustrating the typical environment inhabited by the two lizard species. (The provincial administrative boundary data of China and the geographic map were obtained from the Resource and Environmental Science Data Registration and Publication System and the built-in geographic base map service of ArcGIS Pro software, respectively).

Table 1. Detailed information on primers used for amplifying different target regions by PCR in the present study.

Gene	Primer name	Sequence (5'→3')	Ref.
18S	*Nem_18S*_F	CGCGAATRGCTCATTACAACAGC	[41]
	*Nem_18S*_R	GGGCGGTATCTGATCGCC	
28S	*28S_D2*_F	CGTGTTGCTTGATAGTGCAGC	[42]
	*28S_D2*_R	TTGGTCCGTGTTTCAAGACGG	
COI	*COISKR*_F	TTTTTATGGTGATACCTATT	[18]
	*COISKR*_R	TAGTATTAAAATTACGATCAA	

Phylogenetic analyses

Sequenced fragments were assembled and proofread using DNAMAN 9.0. The resulting sequences were subjected to BLAST searches (https://blast.ncbi.nlm.nih.gov/Blast.cgi) against the NCBI database (www.ncbi.nlm.nih.gov/genbank). Phylogenetic reconstruction was performed based on a concatenated dataset (*18S* + *28S* + *COI*) and mitochondrial *COI* sequence under both Bayesian inference (BI) and maximum likelihood (ML) criteria using PhyloSuite v1.2.2, respectively, implemented in MrBayes and IQ-TREE[43]. *Gyrinicola batrachiensis* Walton, 1929 (Oxyurida: Pharyngodonidae) was designated as the outgroup. The ingroup included 11 species representing two genera within *Spauligodon* and *Skrjabinodon*. Detailed information on the nematode species included in the phylogenetic analysis is provided in Supplementary Table S2. The optimal nucleotide substitution model for the sequences was selected according to the Bayesian information criterion (BIC). The best-fit partitioning scheme and substitution models for IQ-TREE 2.1.2 were determined using the ModelFinder module. Bayesian analysis was implemented in MrBayes 3.2.7, with four independent Markov Chain Monte Carlo (MCMC) chains, each run for 5 × 10^7 generations and sampled every 1,000 generations. To ensure convergence, the first 25% of the samples were discarded as burn-in. ML analysis was performed in IQ-TREE using the Ultrafast Bootstrap (UFBoot) method with 1,000 replicates. The BI trees were evaluated with 5 million generations, while the reliability of the ML trees was assessed using 1,000 bootstrap replicates. For the BI trees, Bayesian posterior probability (BPP) values ≥ 0.98 were considered to indicate strong nodal support, whereas values ≥ 0.95 and < 0.98 indicated moderate support. For the ML trees, bootstrap support (BS) values ≥ 80% were interpreted as strong branch support, while values ≥ 50% and < 80% indicated moderate support. All phylogenetic trees were visualized and annotated using the Interactive Tree of Life (iTOL) v7 platform (https://itol.embl.de/)[13]. Nucleotide polymorphism was analyzed using the DNA Sequence Polymorphism v6.12.01. Inter-specific genetic distances were estimated using MEGA 12.0.

https://doi.org/10.48130/jzser-0026-0002

Nomenclatural acts

The new names contained in this article are available under the International Code of Zoological Nomenclature. This work and the nomenclatural acts it contains have been registered in ZooBank. Zoobank Life Science Identifier (LSID) for this publication is: urn:lsid:zoobank.org:pub: 7707DDA2-9393-4CBA-904A-6F7C147962B3. The LSID registration and any associated information can be viewed in a web browser by adding the LSID to the prefix https://zoobank.org/.

Results

Species identification

Among the observed nematodes obtained from *Eremias roborowskii* and *Teratoscincus roborowskii* in the Turpan Basin, two undescribed species are represented. The morphological characteristics of these two species are described in the following sections.

Spauligodon turpanoeremius *sp. nov.*

Type host: *Eremias roborowskii* Bedriaga, 1912 (Squamata: Lacertidae).

Type locality: Yilahu Town, Tuokexun County (88°27' N, 42°50' E) and Kumtag Desert, Shanshan County (90°23' N, 42°52' E), Turpan City, Xinjiang Uygur Autonomous Region, China.

Additional localities: Gaochang District (89°5' N, 42°58' E) and Tuokexun County (88°52' N, 42°51' E), Turpan City, Xinjiang Uygur Autonomous Region, China.

Site in host: intestine.

Prevalence: 19 of 56 *Eremias roborowskii* examined (33.9%).

Mean intensity of infection (range): 23.47 (2–169) parasites per host.

Type specimens: holotype, adult male (24F00015BQN); allotype, adult female (24F000193qT); paratypes: 10 adult males and 10 adult females (24F0001gW5V~24F0001Ll5k and 24F0001QCLV~24F0001ySDA).

Representative DNA sequences: representative genetic data were deposited in the National Center for Biotechnology Information (NCBI) database (www.ncbi.nlm.nih.gov) under the accession numbers: PV607254, PV607255, PV607259 (*18S*); PV627855, PV627856, PV627857 (*28S*); and PV610208, PV610212 (*COI*).

ZooBank registration: the LSID of the article is urn: lsid: zoobank.org: pub: 7707DDA2-9393-4CBA-904A-6F7C147962B3. The LSID for the new name *Spauligodon turpanoeremius* is urn: lsid: zoobank.org: act: A8AE3AC6-7888-4E7A-899D-79C2846C362A.

Etymology: the new species is named after the type locality and the generic name of its host species.

General description: Small-sized, fusiform nematodes, tapering at both ends. Sexually dimorphic. Males approximately one-third the length of females, with a truncated cephalic end. Cuticle with distinct transverse striations, starting at the anterior end and extending until the caudal extremity. Esophagus cylindrical, surrounded by the nerve ring in its anterior portion, and terminates in a well-developed, valvulated bulb. Esophageal bulb separated from the esophageal corpus by a small constriction. Excretory pore postbulbar, in the shape of a transverse slit. The posterior part of the tail gradually tapered into an elongated, aspinose filament. Lateral alae present in males, absent in females (Figs 3a–j, 4a–q, 5a–j).

Male (based on the holotype and 10 paratypes): body length 1,892.71–2,908.41 (2,228.61 ± 137.69), maximum width 174.97–389.67 (276.29 ± 28.23). Cephalic end with a rounded mouth opening surrounded by six irregular labial flaps; each lip flanked symmetrically by a single amphid; cephalic papillae not seen (Figs 3g, 5a, b). Narrow lateral alae present anteriorly, originating anterior to the nerve ring and extending anterior to the border of caudal alae, divided into two or three sections (Figs 3f, h, 4e, o). Esophagus 310.63–457.82 (372.42 ± 20.98) in total length; corpus length 208.37–331.97 (253.83 ± 16.75); isthmus length 30.20–39.03 (33.01 ± 1.18); bulb length 74.15–118.02 (93.94 ± 7.88) and width 67.02–108.83 (84.33 ± 6.32). Nerve ring at the first third of the esophagus (Figs 3f, 4j), 101.61–117.40 (110.10 ± 3.26) from the anterior end. Excretory pore postbulbar (Figs 3f, 4e, n), 479.92–782.58 (582.71 ± 54.17) from the anterior end. Single tubular testis reflexed immediately posterior to the excretory pore (Fig. 3f). Tail conical, with slight caudal alae projected at both sides, starting at the end of the lateral alae and extending to the posterior of the anal margin (Figs 3j, 4p, 5i). Three pairs of caudal papillae present: the first preanal pair of short-stem papillae situated on slightly inflated portion of the anterior of the anus, enclosed by caudal alae and directed laterally; the second adanal pair of small sessile papillae situated near the end of the caudal alae, enclosed and directed ventrolaterally; the third postanal pair of pedunculated papillae situated at the base of the tail filament, in contact but not enclosed by caudal alae and directed outward; preanal and postanal papillae well developed (Figs 3j, 5i, j). Genital cone large and prominent, situated in the mid-ventral line and surrounded by a pleated membranous curtain (Figs 3j, 5h, i). Spicule 60.16–94.67 (73.10 ± 7.48), proximally robust and distally pointed, absent in some specimens (Figs 3h, i, 4o–q). Caudal extremity ends elongated, posterior end extending into an aspinose filiform tail from postanal papillae (Figs 3f, h, j, 4e, p), 198.58–316.82 (263.64 ± 16.71) long.

Female (based on the allotype and 10 paratypes): body length 2,336.99–3,261.60 (2,732.77 ± 109.64), maximum width 185.55–602.69 (289.51 ± 16.66). Cephalic end with a triangular mouth opening surrounded by three lips, comprising one dorsal lip and two ventrolateral lips. Each lip is incompletely divided into two lobes with a shallow midline indentation. Mouth opening surrounded by three slightly bilobed lips. One small sessile amphid on each ventrolateral lip; cephalic papillae not seen (Figs 3b, 5c, d). Esophagus 470.89–626.72 (543.11 ± 16.19) in total length; corpus length 354.67–480.21 (412.76 ± 12.91); isthmus length 35.75–48.14 (40.64 ± 1.20); bulb length 53.39–156.08 (114.53 ± 4.11) and width 51.50–139.07 (102.29 ± 4.18). Nerve ring at the first third of the esophagus (Figs 3a, 4f, g, i), 103.86–227.09 (132.54 ± 7.42) from the anterior end. Excretory pore postbulbar, 254.63–726.24 (530.08 ± 24.00) from the anterior end. Vulva slightly posterior to excretory pore, as a transverse slit, situated at approximately the first quarter of body, 281.25–804.75 (582.23 ± 33.41) from the cephalic end (Figs 3a, c, 4f, k). Thick-walled muscular ovijector extends posteriorly, continuing as a thin-walled vagina joining two uteri with eggs, both directed posteriorly and parallel to one another, reaching the posterior end before turning anteriorly, not reaching the anus; uteri continue anteriorly to the oviducts, uterus seen only in nongravid females and females with few eggs. In larger females filled with eggs, the internal structures are not visible (Figs 3a, c, 4c, f, k, l). Eggs asymmetrical, 140.02–164.10 (155.10 ± 3.41) in length and 33.17–47.46 (40.17 ± 2.00) in width; slightly flattened on one side; barrel-shaped with a small knob at one end, ends truncated; surface smooth and shell thin, containing blastomeres (Figs 3d, 4d, m, 5g). Tail tapered posteriorly into a conical shape, gradually attenuating toward the caudal extremity (Figs 3a, e, 4a, c, 5e); tail filament 362.29–635.14 (479.74 ± 14.16) long.

Spauligodon turpanoscincus *sp. nov.*

Type host: *Teratoscincus roborowskii* Bedriaga, 1906 (Squamata: Lacertidae).

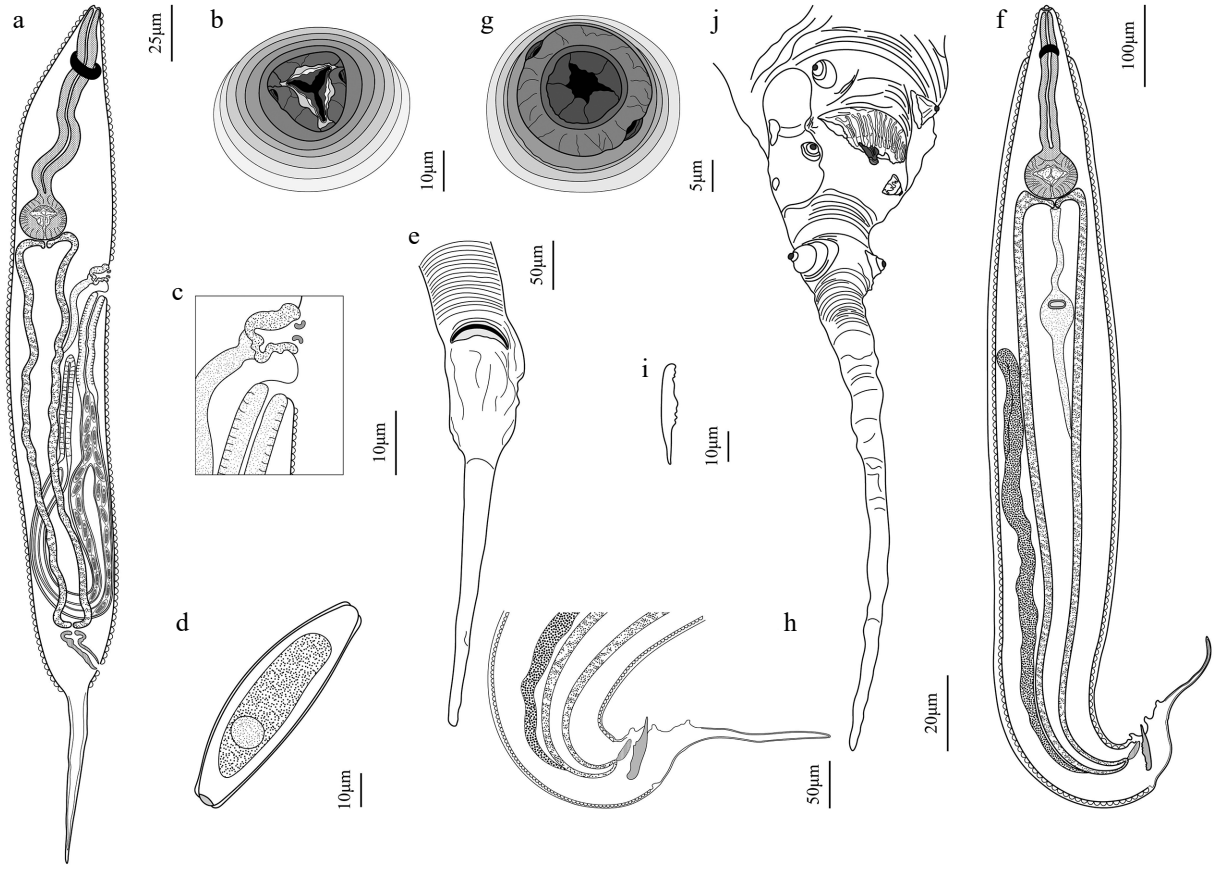

Fig. 3 *Spauligodon turpanoeremius* sp. nov. (a)–(e) female, and (f)–(j) male. (a) Female, gravid, entire, ventral view; (b) en-face view; (c) excretory pore and vulva region; (d) egg; and (e) posterior end, ventral view. (f) Male, entire, lateral view; (g) en-face view; (h) posterior end with spicule, lateral view; (i) spicule; and (j) caudal extremity, ventral view.

Type locality: Yilahu Town, Tuokexun County (88°24' N, 42°50' E), Turpan City, Xinjiang Uygur Autonomous Region, China.

Additional localities: Gaochang District (89°11' N, 42°51' E) and Kumtag Desert, Shanshan County (90°21' N, 42°51' E), Turpan City, Xinjiang Uygur Autonomous Region, China.

Site in host: intestine.

Prevalence: 9 of 29 *Teratoscincus roborowskii* examined (31.0%).

Mean intensity of infection (range): 78.67 (10–300) parasites per host.

Type specimens: holotype, adult male (24F0001Ociy); allotype, adult female (24F0001E7Wo); paratypes: 10 adult males and 10 adult females (24F0001koAD~24F0001m8Jn and 24F0001MgHN~24F0001aS6D).

Representative DNA sequences: representative genetic data were deposited in the National Center for Biotechnology Information (NCBI) database (www.ncbi.nlm.nih.gov) under the accession numbers: PV940946, PV940947 (*18S*); PV940949, PV940950 (*28S*); PV976188, and PV976190 (*COI*).

ZooBank registration: the LSID of the article is urn: lsid: zoobank.org: pub: 7707DDA2-9393-4CBA-904A-6F7C147962B3. The LSID for the new name *Spauligodon turpanoscincus* is urn: lsid: zoobank.org: act: 91C170A3-F2EF-4E66-A0AD-B49857DAE9DF.

Etymology: the new species is named after the type locality and the generic name of its host species.

General description: Small-sized, fusiform nematodes, tapering at both ends. Sexually dimorphic. Males approximately one-third the length of females, with a truncated cephalic end. Cuticle with distinct transverse striations more marked in males, starting at the anterior end and extending until the caudal extremity. Lateral alae present in males and females. Esophagus cylindrical, surrounded by the nerve ring in its anterior portion; the anterior portion of the esophagus ends was constricted, and terminates in a moderately developed bulb with a minute valve. Esophageal bulb separated from the esophageal corpus by a small constriction. Excretory pore postbulbar (prebulbar in developing females), in the shape of a transverse slit. The posterior part of the tail gradually tapered into an elongated, aspinose filament (Figs 6a–j, 7a–o, 8a–r).

Male (based on the holotype and 10 paratypes): body length 1,035.68–1,738.97 (1,318.08 ± 74.45), maximum width 54.70–150.23 (93.41 ± 6.87). Cephalic end with a hexagonal mouth opening surrounded by six equal trapezoidal labial flaps; a pharyngeal denticle was clearly observed internally, situated anterior to the esophagus opening; each lip flanked symmetrically by a single amphid; cephalic papillae not seen (Figs 6b, 8a–c). Robust lateral alae, originating anterior to the nerve ring and extending anterior to the border of caudal alae before narrowing (very narrow lateral alae at its start, but progressively extending along the body) (Figs 6a, c, d, 7c, f, i, 8g). Esophagus 185.61–270.56 (232.87 ± 9.46) in total length; corpus length 121.44–194.09 (157.19 ± 8.03); isthmus length 20.28–28.07 (23.96 ± 0.74); bulb length 36.01–59.53 (46.85 ± 1.70) and width 38.22–59.32 (47.93 ± 1.57). Nerve ring at first quarter to third of the esophagus (Figs 6a, 7f), 42.68–66.96 (58.94 ± 3.60) from the anterior end. Excretory pore postbulbar (Figs 6a, 7c, i), 224.13–394.07 (286.26 ± 17.84) from the anterior end. Single tubular testis reflexed immediately posterior to the excretory pore (Figs 6a, 7c, j). Posterior end truncated, well-developed caudal alae projected at both sides, starting at the anterior of

https://doi.org/10.48130/jzser-0026-0002

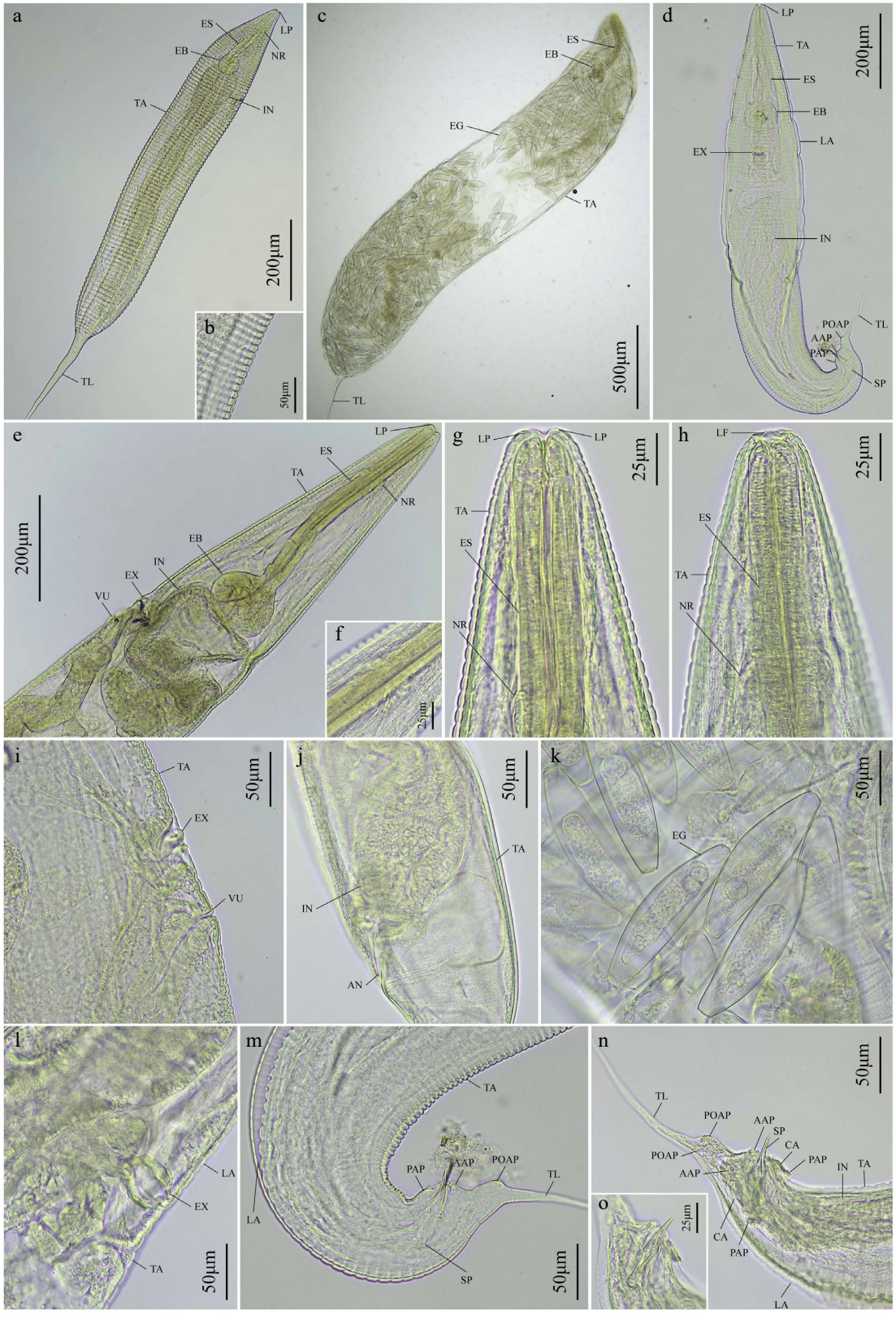

Fig. 4 Digital micrographs of *Spauligodon turpanoeremius* sp. nov. isolated from *Eremias roborowskii*. (a)–(c), (e)–(g), (i)–(k) Female. (d), (h), (l), (m)–(o) Male. (a) Female, whole mount, lateral view; (b) transverse striation of cuticle; (c) female gravid, whole mount, lateral view; (d) male, whole mount, lateral view; (e) female, anterior end, lateral view; (f) nerve ring; (g) cephalic end, ventral view; (h) male, cephalic end, ventral view; (i) female, excretory pore and vulva, lateral view; (j) female, posterior end, ventral view; (k) eggs; (l) male, excretory pore, lateral view; (m) male, posterior end, lateral view; (n) male, caudal morphology, highlighting the spicule, caudal alae, and papillae, ventral view; (o) spicule. AAP, adanal papillae; AN, anus; CA, caudal alae; EB, esophageal bulb; EG, eggs; ES, esophagus; EX, excretory pore; IN, intestine; LA, lateral alae; LF, labial flaps; LP, lips; NR, nerve ring; PAP, preanal papillae; POAP, postanal papillae; SP, spicule; TA, transverse annulations; TL, tail; VU, vulva.

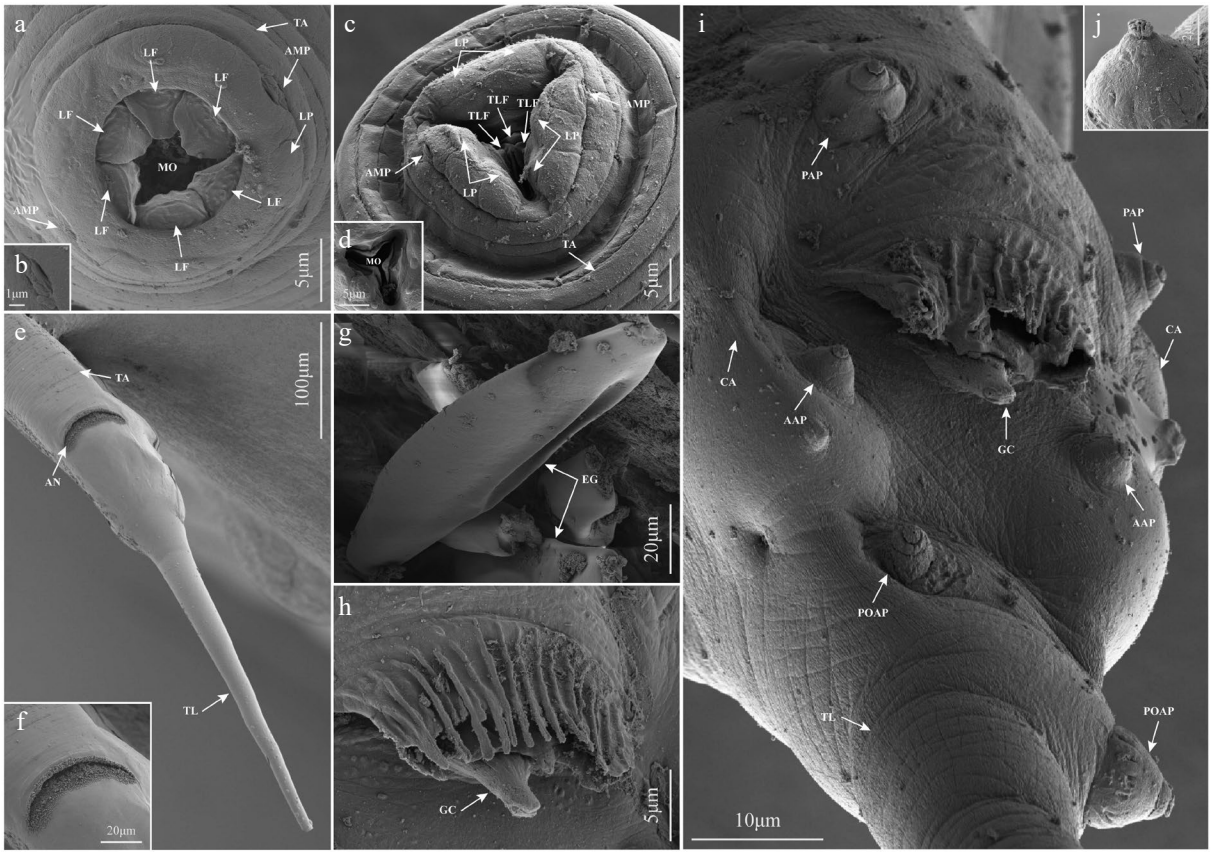

Fig. 5 Scanning electron micrographs of *Spauligodon turpanoeremius* sp. nov. isolated from *Eremias roborowskii*. (a), (b), (h)–(j) Male. (c)–(g) Female. (a) Cephalic end of the male; (b) amphid at the cephalic end; (c) cephalic end of the female; (d) three equal triangular labial flaps and the mouth opening at the cephalic end; (e) smooth caudal region in the female; (f) anus at the caudal region; (g) egg morphology in the female; (h) complex membranous curtain and genital cone in the male anal region; (i) ventral view of the caudal extremity of the male; (j) caudal papillaes. AAP, adanal papillae; AMP, amphid; AN, anus; CA, caudal alae; EG, eggs; GC, genital cone; LF, labial flaps; LP, lips; MO, mouth opening; PAP, preanal papillae; POAP, postanal papillae; TA, transverse annulations; TL, tail; TLF, triangular labial flaps.

the preanal papillae and extending posterior to the postanal papillae (Figs 6a, c, 7c, k, 8k). Three pairs of conspicuous caudal papillae are present: the first preanal pair of short-stem papillae situated on the anterior of the anus, enclosed by caudal alae and directed laterally; the second adanal pair of larger papillae situated near the end of the caudal alae, enclosed and directed ventrolaterally; the third postanal pair of conspicuous pedunculated papillae situated at the base of the tail filament, in contact but not enclosed by caudal alae and directed outward. Two symmetrical slight cone-like processes flank the postanal papillae; adanal and postanal papillae well developed (Figs 6a, c, 7k, 8k, n, o). Genital cone large and prominent, situated in the mid-ventral line and surrounded by a pleated membranous curtain (Figs 6c, 7l, 8k, l). Spicule 48.30–56.05 (52.17 ± 3.88), pointed at both ends and thickened in the middle, absent in some specimens (Figs 6d, e, 7j). The caudal extremity ends are large and robust, the posterior end extending into an aspinose filiform tail from postanal papillae (Figs 6a, c, d, 7c, k), 152.83–276.96 (216.45 ± 9.39) long.

Female (based on the allotype and 10 paratypes): body length 2,268.21–4,365.16 (3,576.47 ± 246.85), maximum width 188.01–515.84 (327.62 ± 20.86). Cephalic end with a triangular mouth opening surrounded by three lips, comprising one dorsal lip and two ventrolateral lips. The dorsal lip is divided into two distinct lobes, whereas the ventrolateral lip is incompletely divided into two lobes with a shallow midline indentation. Two symmetrically arranged small pores are present on each lip. Mouth opening surrounded by three subequal triangular bilobed lips, with tooth-like structures present dorsally on the external lips. One small sessile amphid on each ventrolateral lip; cephalic papillae not seen (Figs 6g, 8d–f). Very tenuous, almost imperceptible, parallel double lateral alae along the body, starting anterior to the excretory pore and extending anterior to the base of the caudal extremity (Figs 6f, h, i, 8h, p–r). Esophagus 480.19–631.27 (537.40 ± 15.55) in total length; corpus length 353.24–480.38 (405.26 ± 12.59); isthmus length 27.41–39.19 (32.50 ± 1.27); bulb length 74.11–136.38 (101.04 ± 3.68) and width 80.76–107.61 (92.95 ± 2.11). Nerve ring at the first quarter to third of the esophagus (Figs 6f, 7e), 82.25–189.01 (114.55 ± 8.09) from the anterior end. Position of the excretory pore varied with developmental stage: prebulbar in developing females, 177.73–364.89 (255.62 ± 39.57) from the anterior end; postbulbar in mature adults, 349.80–621.45 (477.99 ± 28.58) from the anterior end. Vulva slightly posterior to excretory pore, as a transverse slit; the distance from the anterior end measured 205.06–431.84 (301.16 ± 48.27) in the development stage and 417.84–684.58 (536.56 ± 27.76) at the maturation stage (Figs 6f, h, 7a, h, 8i, j). Thick-walled muscular ovijector extends posteriorly, continuing as a thin-walled vagina joining two uteri with eggs, both directed posteriorly and parallel to one another, reaching the posterior end before turning anteriorly, not reaching the anus; uteri continue anteriorly to the oviducts, uterus seen only in nongravid females and females with few eggs. In larger females filled with eggs, the internal structures are not visible (Figs 6f, h, 7a, b, h). Eggs asymmetrical, 140.59–161.32 (150.62 ± 1.44) in length

https://doi.org/10.48130/jzser-0026-0002

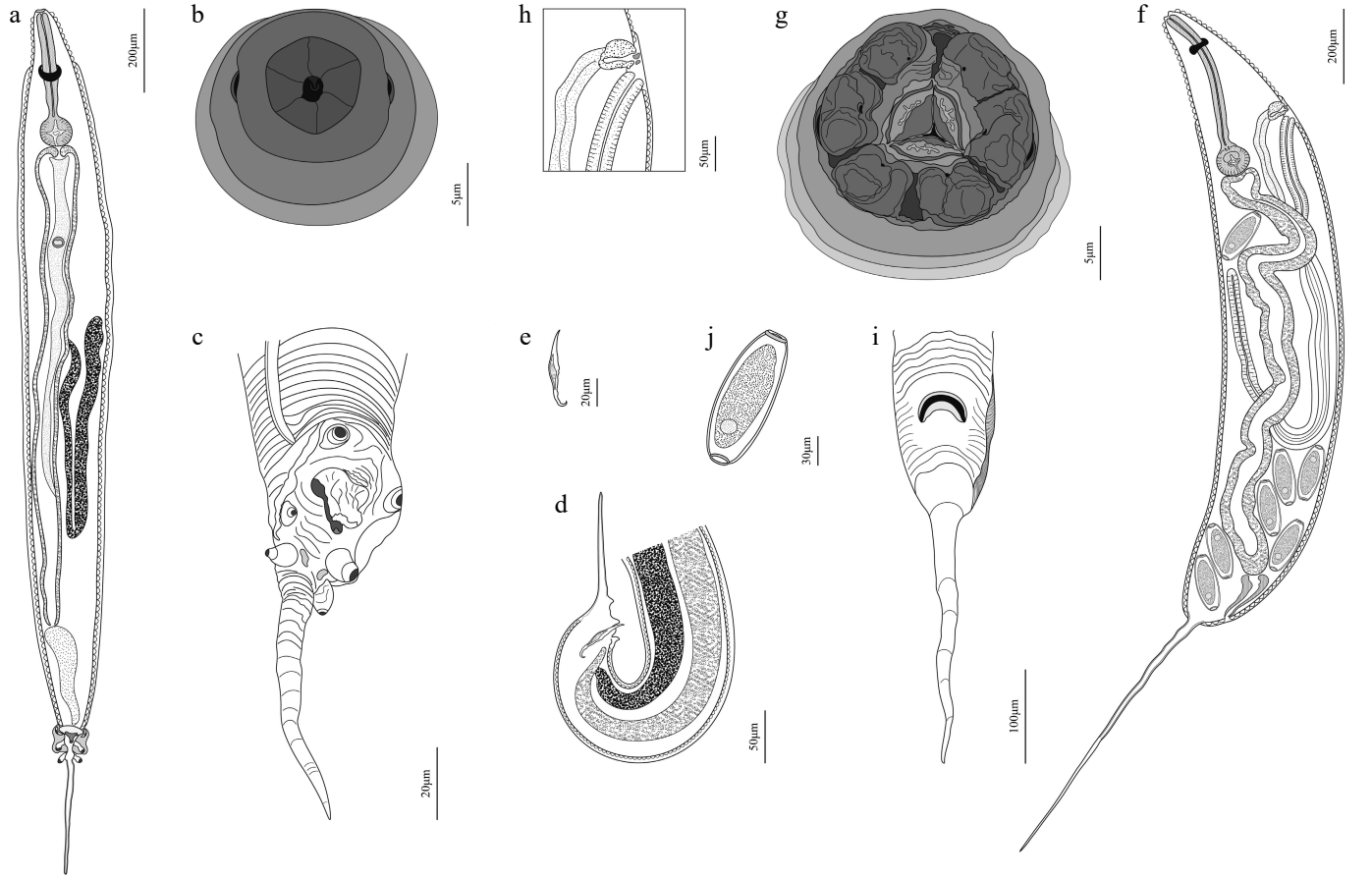

Fig. 6 *Spauligodon turpanoscincus* sp. nov. (a)–(e) Male. (f)–(j) Female: (a) male, entire, ventral view; (b) male, en-face view; (c) male, caudal extremity, lateral view; (d) male, posterior end with spicule, lateral view; (e) spicule. (f) female, gravid, entire, ventral view; (g) female, en-face view; (h) female, excretory pore and vulva region; (i) female, posterior end with lateral alae, ventral view; (j) egg.

and 39.79–56.89 (47.25 ± 1.05) in width; slightly flattened on one side; barrel-shaped with two knobs at the end, ends truncated; surface smooth and shell thin, containing blastomeres (Figs 6j, 7o). Tail tapered posteriorly into a conical shape, gradually attenuating toward the caudal extremity (Figs 6f, i, 7a, m, 8m); tail filament 507.47–1,017.17 (784.69 ± 32.13) long.

Remarks: The overall morphological characteristics of the two novel species allow their assignment to the family Pharyngodonidae: females exhibit a vulva opening situated in the anterior part of the body, just behind the excretory pore, while males possess the posterior pair of papillae not enclosed by the caudal alae, features consistently observed in the genus *Spauligodon* (Supplementary Tables S3, S4)[11]. Consequently, the new species conform to the generic diagnosis of the genus *Spauligodon*, based on the position of the vulva in females and the morphology of the caudal alae in males.

The two novel species identified in this study diverge morphologically from the type species of the genus *Spauligodon, S. extenuatus*, in the following diagnostic characteristics: females possess cephalic papillae, occurrence of lateral alae, vulva situated at level of esophageal bulb, and tail filament with spines; males exhibit broad lateral alae, short and narrow caudal alae, and distinct differences in the morphology and dimensions of the caudal papillae.

Males of the new species *Spauligodon turpanoeremius* sp. nov. possess inconspicuous, bursa-like caudal alae enclosing the preanal and adanal pairs of papillae, resembling conditions observed in *S. aloisei*, *S. atlanticus*, *S. bintangensis*, *S. geckonis*, *S. lamothei*, *S. loboi*, *S. occidentalis*, *S. papuensis*, and *S. xenosauri*. However, females of those species bear 1–9 spines on the tail filament, or males possess 1–7 spines. In contrast, the new species, *Spauligodon nicolauensis*, *S. sharpiloi,* and *S. tectipenis* exhibit an elongated, smooth tail filament in females and lack spines on the tail filament in males. Additionally, the new species possesses a single conspicuous spicule, while it is absent in *Spauligodon nicolauensis*, *S. sharpiloi,* and *S. tectipenis*. *Spauligodon nicolauensis* further differs from the new species in the morphology and size of the three pairs of caudal papillae in males: its first pair is prominently pedunculated, the second pair is large with thick, large peduncles, and the third pair is smaller than the second; in the new species, the first pair is short-stem, the second pair is a smaller sessile papillae, and the third pair is prominently pedunculated. Although *Spauligodon sharpiloi* exhibits numerous morphological differences from the new species, the most pronounced distinction lies in the male lateral alae: it possesses narrow double lateral alae, whereas the new species bears only a single broad lateral alae. Hence, the new species is morphologically distinct from the type species and other congeners of *Spauligodon*.

Males of the new species *Spauligodon turpanoscincus* sp. nov. possess well-developed caudal alae supported by the preanal and adanal pairs of papillae, enabling its clear differentiation from all aforementioned congeners, including the co-described *S. turpanoeremius* sp. nov. It shares greater morphological affinity with species such as *Spauligodon aspiculus*, *S. auziensis*, *S. blydeensis*, *S. bonairensis*, *S. caxiuana*, *S. giganticus*, *S. hemidactylus*, *S. mearnsi*, and *S. persiensis*. However, females of those species either lack lateral alae or males exhibit broad lateral alae that reach their maximum width on the

Fig. 7 Digital micrographs of *Spauligodon turpanoscincus* sp. nov. isolated from *Teratoscincus roborowskii*. (a)–(c), (f), (h), (j) Female. (d), (e), (g), (i), (k), (l), (m) Male: (a) female, whole mount, lateral view; (b) anus, lateral view; (c) female, gravid, whole mount, lateral view; (d) male, whole mount, ventral view; (e) transverse striation of cuticle; (f) female, cephalic end, ventral view; (g) male, cephalic end, ventral view; (h) female, excretory pore and vulva, lateral view; (i) male, esophageal bulb, intestine and excretory pore, ventral veiw; (j) eggs; (k) male, caudal morphology, caudal alae and papillaes, ventral view; (l) highlighting the genital cone, lateral view; (m) male, posterior end, lateral view. AAP, adanal papillae; AN, anus; CA, caudal alae; EB, esophageal bulb; EG, eggs; ES, esophagus; EX, excretory pore; GC, genital cone; IN, intestine; LA, lateral alae; LP, lips; NR, nerve ring; PAP, preanal papillae; POAP, postanal papillae; SP, spicule; TA, transverse annulations; TL, tail; VU, vulva.

anterior portion of the anus. In contrast, the new species, *Spauligodon tarentolae* and *S. timbavatiensis,* possess lateral alae in females and narrow lateral alae in males. The new species can be readily distinguished from *Spauligodon tarentolae* and *S. timbavatiensis* following these characteristics: the second and third pairs of papillae in males of the new species are pedunculated, whereas those of *S. tarentolae* are long-pedunculated; females of the new species exhibit a dorsal lip with two distinct lobes and ventrolateral lips with two incomplete lobes, whereas all lips are divided into two distinct lobes in *S. timbavatiensis*. Hence, the new species is morphologically distinct from the type species and other congeners of *Spauligodon*.

Key to the species of the genus Spauligodon based on phylogenetic analyses

1) Double lateral alae in males	***Spauligodon sharpiloi***
1.1) Single lateral alae in males	**2**
2) Tail filament with 1–5 spines in males	***Spauligodon carbonelli***
2.1) Caudal filament in males lack spines	**3**
3) Mouth opening with a cephalic papillae on each of six labial flaps, two symmetrically arranged amphids present lateral to the lips in males	***Spauligodon auziensis***
3.1) Mouth opening without cephalic papillaes on each of six labial flaps, two symmetrically arranged amphids present lateral to the lips in males	**4**

https://doi.org/10.48130/jzser-0026-0002

4) Mouth opening with a pair of setiform erect cephalic papillae on each of three labial flaps, two symmetrically arranged amphids present lateral to the lips in females; a pair of short-stem papillae at the base of tail filament in males	***Spauligodon extenuatus***
4.1) Mouth opening without cephalic papillaes on each of three labial flaps, two symmetrically arranged amphids present lateral to the lips in females; a pair of prominent and pedunculated papillae at the base of tail filament in males	**5**
5) Cephalic end with three slightly bilobed lips in females	**6**
5.1) Cephalic end with three conspicuously bilobed lips in females	**7**
6) Vulva situated in the anterior of the esophageal bulb just behind the excretory pore in females	***Spauligodon atlanticus***
6.1) Vulva situated in the posterior of the esophageal bulb just behind the excretory pore in females	***Spauligodon nicolauensis***
7) Males approximately half the length of females; lateral alae reaching maximum width on the anterior of the anus; a pair of pedunculated papillae present the anterior to the anus, postanal papillae larger than the first pair	***Spauligodon occidentalis***
7.1) Males approximately one-third the length of females; lateral alae terminating the anterior to the anus; a pair of short-stem papillae present the anterior to the anus, postanal papillae larger than the first pair	**8**
8) Parallel double lateral alae in females, broad caudal alae in males	***Spauligodon turpanoscincus***
8.1) Absence of lateral alae in females; inconspicuous caudal alae in males	**9**
9) Tail filament with 5–9 spines in females; eggs oval	***Spauligodon cabrerae***
9.1) Caudal filament in females lack spines; eggs barrel-shaped	**10**
10) Presence of genital cone and single spicule in males	***Spauligodon turpanoeremius***
10.1) Presence of genital cone but absence of spicule in males	**11**
11) Parasites primarily inhabiting the large intestine	***Spauligodon saxicolae***
11.1) Parasites primarily inhabiting the small intestine	***Spauligodon lacerate***

Molecular characterization

Phylogenetic analysis of Spauligodon turpanoeremius *sp. nov. and* S. turpanoscincus *sp. nov.*

The *18S* sequences of *Spauligodon turpanoeremius* sp. nov. obtained herein are 870–882 bp in length with 2.2% nucleotide divergence, representing three different genotypes. The *28S* sequences are 595–610 bp in length with 0.1% nucleotide divergence, representing two different genotypes. The *COI* sequences are 452–453 bp in length with no nucleotide polymorphism detected. Pairwise comparison of the *18S*, *28S*, and *COI* sequences of *Spauligodon turpanoeremius* sp. nov. with those of *Spauligodon* spp. displayed 0.1% to 2.3%, 3.0% to 6.1%, and 8.7% to 12.1% nucleotide divergence.

The *18S* sequences of *Spauligodon turpanoscincus* sp. nov. obtained herein are 920–937 bp in length with no nucleotide polymorphism detected. The *28S* sequences are 624–634 bp in length with 0.2% nucleotide divergence, representing two different genotypes. The *COI* sequences are 450–451 bp in length with 0.9% nucleotide divergence, representing two different genotypes. Pairwise comparison of the *18S*, *28S*, and *COI* sequences of *Spauligodon turpanoscincus* sp. nov. with those of *Spauligodon* spp. displayed 1.2% to 1.6%, 1.2% to 10.4%, and 9.0% to 13.3% nucleotide divergence.

Phylogenetic trees reconstructed from the obtained concatenated (*18S* + *28S* + *COI*) sequence data of pharyngodonid nematodes from *Eremias roborowskii* and *Teratoscincus roborowskii* using the Bayesian inference (BI) and maximum likelihood (ML) methods exhibited high topological congruence and consistently revealed that *Spauligodon turpanoeremius* sp. nov. and *S. turpanoscincus* sp. nov. formed two distinct monophyletic clades, separate from other congeneric species within *Spauligodon* (Fig. 9). In the concatenated dataset analyzed under the BI and ML methods with *Gyrinicola batrachiensis* designated as the outgroup, the representatives of the family Pharyngodonidae were divided into two major clades. Clade I consisted of representatives of the Pharyngodonidae, as well as *Spauligodon turpanoeremius* sp. nov. and *S. turpanoscincus* sp. nov. identified in this study; Clade II contained only one undetermined species of the genus *Spauligodon, Spauligodon* sp. In Clade I, *Spauligodon turpanoscincus* sp. nov. formed a separate branch with strong support in BI and ML trees (BPP = 0.98; BS = 87). Meanwhile, other species of *Spauligodon* and *Skrjabinodon* from Clade I clustered together with *Spauligodon* sp. from Clade II to form a larger clade; however, the species within Clade I were further subdivided into several distinct and stable subclades that were strongly supported in the BI tree but moderately supported in the ML tree. *Spauligodon auziensis* stood apart from other species and formed a distinct subclade with strong support in BI and ML trees (BPP = 1; BS = 99). Furthermore, *Spauligodon turpanoeremius* sp. nov. also formed an independent branch within a subclade of Clade I, exhibiting extremely strong support in BI and ML trees (BPP = 1; BS = 96). Notably, *Skrjabinodon poicilandri* (Pharyngodonidae) may be erroneously nested within the *Spauligodon* clade, forming a sister relationship to other species of *Spauligodon* with weak support in BI and ML trees. *Spauligodon carbonelli* + *S. atlanticus* + *S. lacertae* + *S. cabrerae* + (*S. occidentalis* + *S. extenuatus*) formed a subclade that was strongly supported in the BI tree, but moderately supported in the ML tree (BPP = 1; BS = 76); this subclade further clustered with *S. nicolauensis* + *S. saxicolae* to form a larger subclade that was weakly supported in the BI and ML trees. Accordingly, the sequences of the species described in this study belong to the genus *Spauligodon*, forming two distinct clades on the phylogenetic tree that are clearly separated from other species in the genus.

Phylogenetic analysis of the genus Spauligodon

Genetic distances (*p*-distance) for *Spauligodon turpanoeremius* sp. nov. and *S. turpanoscincus* sp. nov. were calculated across *COI* and concatenated sequences (Table 2). The genetic divergence between two new species and their congeners exceeded the interspecific distances observed among other congeneric taxa: based on *COI* sequences, the uncorrected *p*-distance for *Spauligodon turpanoeremius* sp. nov. and *S. turpanoscincus* sp. nov. ranged from 13.05%–21.24% and 13.53%–19.51% greater than the 5.95%–19.61% divergence among the congeneric taxa; and for concatenated sequences, values were 5.84%–9.34% and 7.67%–9.92% vs 2.75%–9.35%.

Furthermore, our analyses revealed that phylogenetic trees reconstructed from the mitochondrial *COI* sequence data using the BI and ML methods had almost identical topologies and strong support for *Spauligodon turpanoeremius* sp. nov. and *S. turpanoscincus* sp. nov. (Fig. 10). Within these phylogenies, species of *Spauligodon* consistently clustered into two distinct clades and were clearly separated from the genus *Skrjabinodon*. Consequently, congeneric species clustered together into a monophyletic clade, thereby permitting the unequivocal differentiation of these morphologically similar genera in molecular phylogenetic analyses and implying divergent evolutionary trajectories. The two newly described species formed a distinct monophyletic clade with sympatric distribution, but *Spauligodon turpanoscincus* sp. nov. demonstrated a longer genetic distance and a higher evolutionary rate compared to *S. turpanoeremius* sp. nov., indicative of substantial sequence divergence between them. An additional issue is

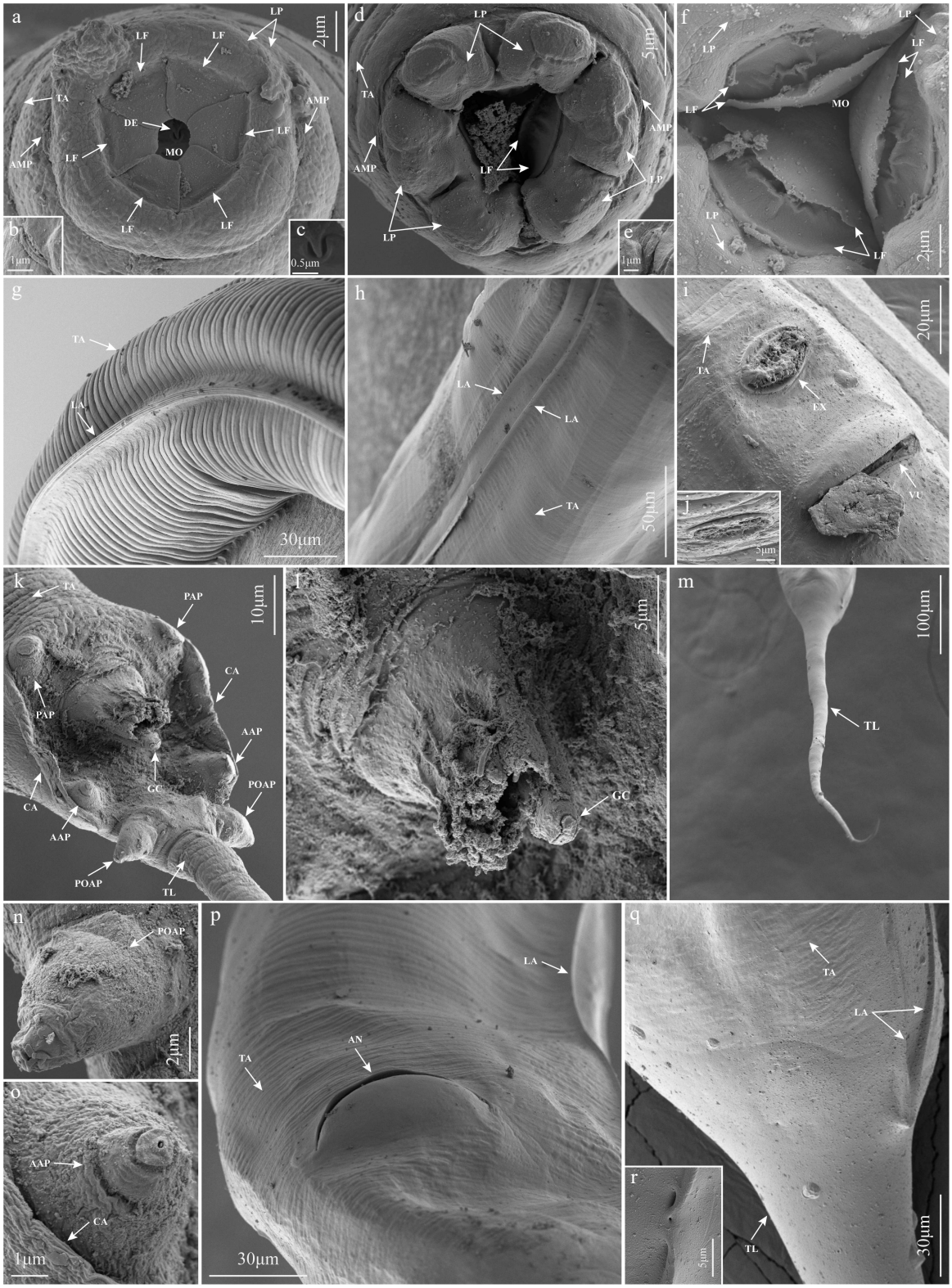

Fig. 8 Scanning electron micrographs of *Spauligodon turpanoscincus* sp. nov. isolated from *Teratoscincus roborowskii*. (a)–(c), (g), (k), (l), (n), (o) Male. (d)–(f), (h)–(j), (m), (p)–(r) Female: (a) cephalic end of the male; (b) amphid at the cephalic end; (c) denticle at the cephalic end in the male; (d) cephalic end of the female; (e) amphid at the cephalic end in the female; (f) three well-developed bilobed labial flaps and the mouth opening at the cephalic end in the female; (g) lateral view of the midbody of the male; (h) lateral view of the midbody of the female; (i) ventral view of the excretory pore and vulva in the anterior region of the female; (j) excretory pore in the female; (k) ventral view of the caudal extremity of the male; (l) complex membranous curtain and genital cone in the male anal region; (m) caudal filament of the female; (n) postanal papillae; (o) adanal papillae; (p) ventral view of the anus in the caudal region of the female; (q) smooth caudal region in the female; (r) termination point of the lateral alae and cuticular pit in the caudal region of the female. AAP, adanal papillae; AMP, amphid; AN, anus; CA, caudal alae; DE, denticle; EX, excretory pore; GC, genital cone; LA, lateral alae; LF, labial flaps; LP, lips; MO, mouth opening; PAP, preanal papillae; POAP, postanal papillae; TA, transverse annulations; TL, tail; VU, vulva.

https://doi.org/10.48130/jzser-0026-0002

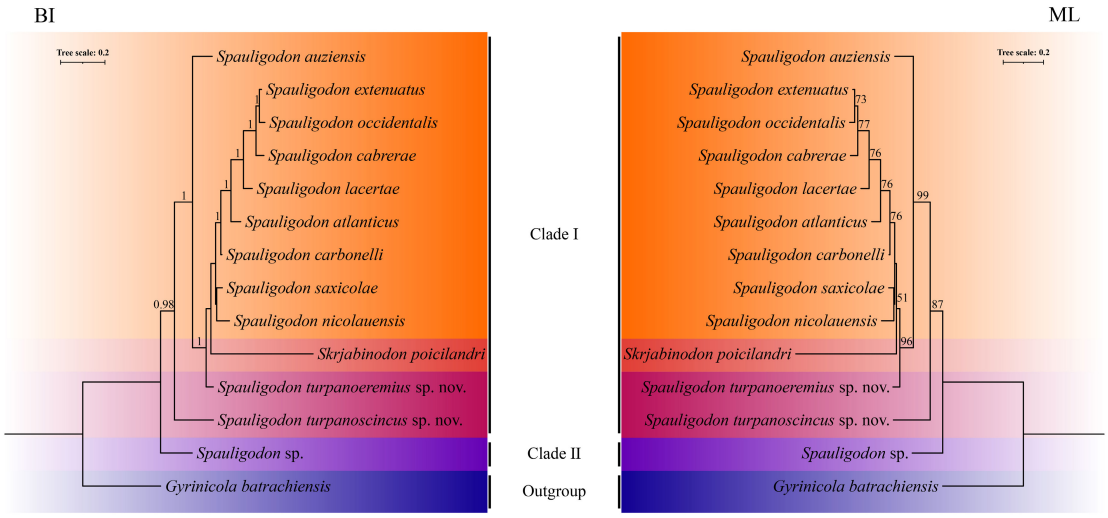

Fig. 9 Bayesian inference (BI) and maximum likelihood (ML) inference based on the concatenated (*18S* + *28S* + *COI*) sequence data shows the phylogenetic relationships among the representatives of Pharyngodonidae, *Spauligodon turpanoeremius*sp. nov. and *S. turpanoscincus*sp. nov.

Table 2. Uncorrected *p*-distance (%) of *Spauligodon turpanoeremius* sp. nov. and *S. turpanoscincus* sp. nov. sequences (*COI* above diagonal; concatenated sequences below diagonal).

	1	2	3	4	5	6	7	8	9	10	11	12	13	14
1. *S. turpanoeremius* sp. nov.		13.75	16.15	21.24	17.81	13.05	15.30	14.38	15.04	16.44	15.04	15.27	26.83	31.42
2. *S. turpanoscincus* sp. nov.	8.46		15.96	19.51	17.62	13.53	16.02	16.41	16.63	16.02	17.74	15.08	27.91	30.60
3. *S. atlanticus*	7.50	8.54		18.86	15.88	5.95	12.04	12.38	19.61	13.79	15.43	12.38	29.00	30.39
4. *S. auziensis*	9.34	9.92	9.35		21.36	18.17	19.15	18.17	19.03	20.23	21.11	17.82	30.89	29.93
5. *S. cabrerae*	7.85	9.30	3.78	9.58		14.49	13.96	13.96	18.15	14.66	17.98	14.14	29.27	31.76
6. *S. carbonelli*	6.31	7.67	2.75	8.46	4.69		12.91	10.61	18.49	13.61	15.27	11.74	29.27	30.71
7. *S. extenuatus*	7.09	8.89	3.37	9.64	3.25	4.22		8.73	17.80	10.82	15.88	12.22	29.81	30.37
8. *S. lacertae*	7.03	9.01	3.25	9.40	3.08	3.93	1.92		17.36	10.65	15.11	12.38	28.46	28.78
9. *S. nicolauensis*	7.81	8.59	8.27	8.75	8.22	7.54	7.86	7.86		19.37	18.81	17.20	26.56	30.23
10. *S. occidentalis*	7.32	9.01	3.31	9.63	3.60	4.51	2.56	2.61	7.92		17.10	12.39	28.46	30.19
11. *S. saxicolae*	5.84	8.43	5.39	8.75	5.98	4.98	5.51	5.22	7.07	5.92		17.36	28.46	29.42
12. *Spauligodon* sp.	7.75	8.75	7.42	5.61	7.48	6.82	7.07	7.25	8.16	7.07	7.05		27.64	29.26
13. *Skrjabinodon poicilandri*	16.81	17.77	18.05	18.33	18.05	17.32	18.35	17.99	17.45	18.04	16.97	17.75		34.96
14. *Gyrinicola batrachiensis*	20.01	20.70	20.30	20.53	20.60	19.83	20.48	19.88	19.70	20.77	19.28	20.24	21.79	

that a notable incongruence emerged between morphology and phylogeny. For instance, despite their close phylogenetic affinity, *Spauligodon auziensis* and *S. nicolauensis* exhibit marked morphological differentiation: males of *S. auziensis* possess broad lateral alae and caudal alae, pedunculated papillae, and the presence of a spicule, with females featuring lateral alae and spindle eggs; in contrast, males of *S. nicolauensis* are characterized by narrow lateral alae and caudal alae, prominently pedunculated papillae, and absence of a spicule, with females lacking lateral alae and lanceolate eggs. Similar discordances were observed for other species pairs: *Spauligodon saxicolae* and *S. carbonelli*, *S. lacertae* and *S. extenuatus*, all of which were phylogenetically proximate yet morphologically distinct. Conversely, although the species pair between *Spauligodon atlanticus* and *S. occidentalis* exhibited considerable morphological similarity, they were positioned distantly within the phylogenetic tree. An analogous pattern was observed for *Spauligodon saxicolae* and *S. lacertae*.

Discussion

Spauligodon represents the most speciose genus within the family Pharyngodonidae. Although Pazoki et al.[5] and Hodda[25] recorded 50 and 44 described *Spauligodon* species, respectively, the genus is generally considered to comprise 57 recognized species, 17 of which have been documented in the Palaearctic realm[7,8,11,44]. The newly described *Spauligodon turpanoeremius* and *S. turpanoscincus,* both originating from the Palaearctic realm, represent the 18th and 19th species recorded from this biogeographic zone and are designated as the 58th and 59th valid species within the genus.

Traditionally, the delineation within the genus *Spauligodon* is based on the presence or absence of the spicule in males, the occurrence of spines on the tail filament of adults, egg morphology, and geographical distribution[45]. The genus *Skrjabinodon* shows a close phylogenetic affinity to *Spauligodon*, with primary diagnostic characteristics including size, morphology, number of spines on the caudal extremity, number of caudal papillae, and egg morphology[19]. In many cases, the taxonomy remains predominantly morphology-based. Although species of *Skrjabinodon* are generally morphologically similar to *Spauligodon*, males of the former can generally be distinguished by the absence of caudal alae and the presence of sessile, frequently reduced papillae. Contrastingly, the females of these two genera typically lack reliably differential morphological characteristics for generic discrimination, which represents a source of taxonomic ambiguity[21]. For instance, Castillo et al.[46] assigned *Spauligodon castillensis* to *Skrjabinodon* based solely on the absence of caudal alae in males, utilizing tail filament morphology, number of spines, and geographical distribution as

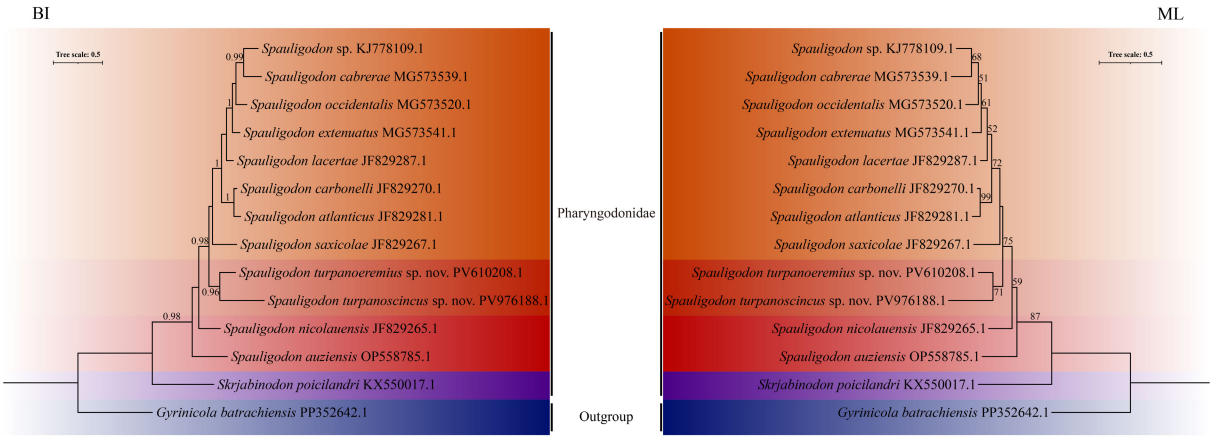

Fig. 10 Phylogenetic relationships between *Spauligodon turpanoeremius* sp. nov. and *S. turpanoscincus* sp. nov. inferred from *COI* sequences using Bayesian inference (BI) and maximum likelihood (ML) methods.

key characteristics to differentiate it from other congeners. Correspondingly, species identification in *Spauligodon* is largely dependent on alternative male characteristics, notably morphological differences in the caudal papillae and the genital cone[2,15]. For example, *Spauligodon occidentalis* and *S. atlanticus* have extremely similar male and female characteristics, differing only in the size and shape of the three pairs of caudal papillae in males[47]. To rectify current ambiguities in taxonomic assignment, we sought to revise the generic key for *Spauligodon*, including the incorporation of supplementary morphological evidence.

The males of the genus *Spauligodon* are characterized by pronounced male dimorphism, with two distinct male morphotypes within a single species. One of these morphotypes has the typical *Spauligodon* phenotype, featuring caudal alae supported by postanal papillae, well-developed pedunculate papillae, and a genital cone, whereas the other lacks caudal alae and a genital cone, has reduced sessile papillae, and bears a spicule—features that morphologically bear a close resemblance to those of *Skrjabinodon*[21]. This phenomenon represents a considerable challenge with respect to traditional taxonomic practices primarily based on male morphological characteristics for species identification. Nevertheless, genetic analyses of *Spauligodon saxicolae* and related species by Jorge et al.[21] have confirmed that despite marked morphological disparities, both male morphotypes belong to the same species, thereby indicating that male dimorphism represents intra-specific variation within the genus rather than serving as a means for distinguishing discrete species. Consequently, in assessments of the taxonomy of *Spauligodon* and related genera, it is imperative to carefully consider the implications of male dimorphism in their classification frameworks. The morphological features of the two new species described in this study are consistent with this phenomenon, further emphasizing that the presence of male dimorphism, coupled with insufficient diagnostic characteristics, may lead to erroneous generic assignment of a species to a closely related genus. Given these considerations, comprehensive examinations based on scanning electron microscopy, focusing on lip morphology and number of labial flaps, the position, number, and morphology of the amphid, lateral alae configuration, pleated membranous curtain of the genital cone, size and shape of male caudal papillae, and degree of caudal alae development, can provide key diagnostic criteria to minimize taxonomic misidentification. Moreover, these features can be augmented by combining with comparative morphological analysis of key diagnostic characters, including body dimensions, the start and end of the lateral alae, esophageal and bulb dimensions, distances from the anterior end to the nerve ring, excretory pore and vulva, spicule length, and the number of spines on the tail filament[5].

In addition to the aforementioned inaccuracies in species identification, the current paucity of genetic data for the Pharyngodonidae has impeded satisfactory resolution of the phylogenetic relationships among these taxa[18,21,32,48], thereby presenting a major obstacle to elucidating the evolutionary history of this taxon[49]. Research conducted to date on *Spauligodon* has focused primarily on morphological descriptions and comparisons, with a notable paucity of molecular phylogenetic data. This lack of data not only hinders the clarification of infrageneric relationships and accurate description of new species but raises the possibility of cryptic species or taxonomic confusion among taxa described from biogeographical regions[1]. Furthermore, the generic placement and validity of certain species within the genera *Spauligodon* and *Skrjabinodon* remain unclear. Although morphological characterization has been completed for most *Spauligodon* species, genetic characterization remains limited. This paucity of molecular data[11], combined with ambiguous generic diagnostic traits, has resulted in the poorly defined delimitation between *Spauligodon* and *Skrjabinodon*, thereby corroborating the observations of Binh et al.[50]. In the present study, comparative morphological and molecular phylogenetic analyses revealed only minor morphometric divergences from previously described congeners. Moreover, molecular phylogenetic analyses revealed that species of *Spauligodon* and *Skrjabinodon* cluster within a single monophyletic clade comprising independent, albeit closely related, evolutionary lineages, thereby corroborating the conclusions of Mockett et al.[18]. Notably, phylogenetic reconstructions based on the mitochondrial *COI* gene and a nuclear–mitochondrial multigene strategy consistently supported the validity of both *Spauligodon turpanoeremius* and *S. turpanoscincus*, each forming independent lineages distinct from those of other *Spauligodon* species and related pharyngodonid taxa. In addition, all congeners clustered into three subclades, two of which comprise species isolated exclusively from lacertid hosts (with the exception of *Spauligodon nicolauensis*) and one containing only *S. auziensis* derived from phyllodactylid hosts. Our findings are consistent with the conclusions drawn by Ferreira et al.[49], who indicated that *Spauligodon auziensis* and *S. nicolauensis* do not form a monophyletic clade. Paradoxically, as a parasite of lizards in the family Phyllodactylidae, *Spauligodon nicolauensis* was consistently found to be nested within the lacertid-associated clade. This contrasts with the findings of Pereira et al.[1], who placed *Spauligodon auziensis* and *S. nicolauensis* within strongly supported monophyletic clades. Our findings also differ from those of Chabaud et al.[51] and

https://doi.org/10.48130/jzser-0026-0002

Adamson[38], indicating speciation within this pharyngodonid lineage is consistent with host taxonomy rather than geographical distribution. Consequently, this study provides robust support for the phylogenetic placement of *Spauligodon turpanoeremius* and *S. turpanoscincus* within *Spauligodon*, thereby emphasizing that the lineages of pharyngodonid parasites in reptiles have passed through a speciation process led by the host.

On the basis of their divergence in different groups of hosts, Petter[52] and Petter et al.[2] have distinguished two evolutionary lineages among pharyngodonid nematodes. The first lineage includes all Pharyngodonidae of carnivorous saurians, including the genus *Spauligodon*, and the second evolutionary lineage includes the Pharyngodonidae of herbivorous Iguanidae and Testudinidae, comprising various genera such as *Tachygonetria*. In this study, we revealed that species of *Spauligodon* predominantly inhabit the intestinal tracts of carnivorous and omnivorous lizards, and that their morphological characteristics exhibit a discernible correlation with host dietary ecology, indicating that key diagnostic traits in both males and females may undergo modification in response to shifts in host feeding strategies. Nematodes in the genus *Spauligodon* parasitizing carnivorous lizards display pronounced and readily distinguishable morphological characteristics, such as the well-developed caudal papillae characterizing the males of *Spauligodon cubensis* and *S. nicolauensis*[12,48,53]. Similarly, the males of *Spauligodon bonairensis* have broad lateral and caudal alae, with both the males and females bearing spines on the tail filament[54,55], whereas in the males of *S. aloisei* and *S. xenosauri*, the caudal alae are comparatively inconspicuous[6,53,56,57]. The males of *Spauligodon aspiculus* and *S. persiensis* are characterized by broad caudal alae and well-developed caudal papillae, whereas the females of *S. persiensis* additionally exhibit a spinose tail filament[5,11,58], although the males of *S. papuensis* similarly possess these morphological traits but lack conspicuous caudal alae[59,60]. Readily distinguishable lateral and caudal alae along with well-developed caudal papillae are characteristic features used to identify the males of *Spauligodon auziensis*, *S. hemidactylus*, and *S. oxkutzcabiensis*; notably, the females of *Spauligodon hemidactylus* and *S. oxkutzcabiensis* have both lateral alae and a tail filament bearing spines[61–65]. In contrast, the males of *Spauligodon tarentolae* and *S. timbavatiensis* are distinguished solely by the absence of conspicuous lateral alae, and the females of *S. tarentolae* are characterized by an aspinose tail filament[66,67]. Moreover, species including *Spauligodon atlanticus*[47,68], *S. extenuatus*[61,69], *S. lamothei*[70,71], *S. occidentalis*[47,53], and the newly described *S. turpanoscincus* from this study all parasitize omnivorous lizards, which exhibit at least three or more of the distinctive morphological traits representative of those observed in carnivorous host lineages. In comparison, females of the newly described *Spauligodon turpanoeremius* lack lateral alae, whereas the males display reduced lateral and caudal alae, along with underdeveloped diminutive caudal papillae. Furthermore, both females and males possess a tail filament without spines. These observations accordingly provide evidence to indicate that nematodes in the genus *Spauligodon* that parasitize omnivorous lizards have two divergent morphotypes, whereas only one of these is observed in carnivorous host populations. These morphotypes can provisionally be categorized as 'pronounced' and 'general', although the possibility of exceptions to this generalized dichotomy should not be excluded. Consequently, whereas multiple ecological factors—including geographical distribution, reproductive isolation, predatory pressure, and population density—may collectively contribute to shaping the host–parasite association, the phylogenetic congruence between the interacting taxa may merely represent apparent concordance[72,73]. This is consistent with the general consensus that perfect congruence between the two phylogenies is rare[74]. In conclusion, this emphasizes the need for further research to determine whether shifts in the diets of lizards influence the population structure and potential speciation within *Spauligodon*, and whether co-evolutionary relationships have developed between these parasites and their hosts.

Conclusions

In this study, we adopted an integrative taxonomic approach, combining comparative morphological observations and phylogenetic analyses based on the mitochondrial *COI* gene and a multi-gene dataset, to identify and describe two new species of *Spauligodon*: *S. turpanoeremius* sp. nov. and *S. turpanoscincus* sp. nov. These species were respectively identified as intestinal parasites of the desert lizards *Eremias roborowskii* and *Teratoscincus roborowskii*, representing the first records for both of these hosts. In addition, by developing a dichotomous identification key for the genus, we have contributed to reducing the confounding influence of male dimorphism on species diagnosis, thereby substantially enhancing the reliability of morphological identification. Our phylogenetic reconstructions based on the currently available molecular data enabled us to further clarify the taxonomic positions of these species within the genus. Notably, our findings provide empirical support for a host-driven speciation process in *Spauligodon*, indicating a potential co-evolutionary association shaped by host feeding habits and parasite adaptation. Collectively, our findings not only refine the framework for species identification within the genus but also provide broader insights into the systematics and evolutionary mechanisms underpinning parasite diversification.

Ethical statements

The animal study protocol was approved by the Laboratory Animal Welfare and Ethics Committee of Xinjiang Agricultural University (Protocol code 2025019 and date of approval 2025.01.23). Experiments were conducted in compliance with animal ethics guidelines and approved protocols. This work represents the authors' own intellectual contribution, and no AI tool is credited as an author.

Author contributions

The authors confirm contributions to the paper as follows: conceptualization: Jiang Z, Yan X; data curation: Ba Y, Jiang Z, Li S, Liu C, Wang T, Yan X, Zhao Y; formal analysis: Ba Y, Chen S, Jiang Z, Li S, Liu C, Wang T, Zhao Y; funding acquisition: Yan X; investigation: Ba Y, Chen S, Jiang Z, Liu C, Wang T, Yan X; methodology: Ba Y, Chen S, Jiang Z, Liu C, Yan X; project administration: Yan X; resources: Yan X; software: Ba Y, Chen S, Jiang Z, Liu C, Wang T; supervision: Yan X; validation: Ba Y, Chen S, Jiang Z, Liu C, Yan X; visualization: Ba Y, Jiang Z; writing – original draft: Jiang ZQ; writing – review and editing: Yan X. All authors reviewed the results and approved the final version of the manuscript.

Data availability

The data that support the findings of this study are available in the GenBank repository (www.ncbi.nlm.nih.gov). These sequence data generated in this study have been submitted to the GenBank database under accession numbers PV607254-PV607259, PV610208-PV610212, PV627853-PV627857, PV940946-PV940948, PV940949-PV940951, PV976188-PV976190. All data generated and analyzed are included in this published article and its supplementary information files. During the preparation of this work, the authors used ABI PRISM 3730

platform for sequence determination, Adobe Illustrator 28.0 for figure preparation, ArcGIS Pro 3.5.2 for map construction, DNAMAN 9.0 for sequence assembly, concatenation and proofreading, DNA Sequence Polymorphism v6.12.01 for data analysis, Editage platform for language refinement, IBM SPSS Statistics 25 for data calculation, IQ-TREE 2.1.2, MrBayes 3.2.7 and PhyloSuite v1.2.2 for phylogenetic reconstruction, ITOL v7 platform for visualization and annotation, MEGA 12.0 for inter-specific genetic distance estimation, Motic BA210 digital microscope and image acquisition system for morphological observation, NCBI database for BLAST analysis, and Zeiss Supra 55 VP scanning electron microscope for photomicrography. The authors reviewed and edited all content produced with the assistance of this tool, verified its accuracy, and take full responsibility for the integrity and originality of the final manuscript.

Acknowledgments

We thank the Xinjiang Institute of Ecology and Geography, Chinese Academy of Sciences, for technical support. We would like to thank the Editage platform (www.editage.cn) for English language editing.

Funding

This work was supported by the National Natural Science Foundation of China (Grant No. 32460130); the Xinjiang Key Laboratory of Ecological Adaptation and Evolution of Extreme Environment Biology (Grant No. KFKT2401); the Natural Science Foundation of Xinjiang Uygur Autonomous Region (Grant No. 2022D01A194); the Open Research Program of the National Parasite Resource Bank (Grant No. 2019-194-30); and the Third Xinjiang Scientific Expedition Program (Grant No. 2022xjkk1200).

Conflict of interest

The authors declare that there is no conflict of interest regarding the publication of this article.

Supplementary information accompanies this paper online at: https://doi.org/10.48130/jzser-0026-0002.

Dates

Received 15 April 2026; Revised 10 June 2026; Accepted 15 June 2026; Published online 28 July 2026

References

[1] Pereira FB, Luque JL, Tavares LER. 2018. Integrative approach on Pharyngodonidae (Nematoda: Oxyuroidea) parasitic in reptiles: relationship among its Genera, importance of their diagnostic features, and new data on *Parapharyngodon bainae*. *PLoS One* 13(7):e0200494

[2] Petter AJ, Quentin JC. 1976. Keys to the genera of the Oxyuroidea. In *CIH Keys to the Nematode Parasites of Vertebrates*, eds Anderson RC, Chabaud AG, Willmott S. UK: Commonwealth Agricultural Bureaux. 30 pp

[3] Gibbons LM. 2009. *Keys to the nematode parasites of vertebrates: Supplementary volume*. Vol. 10. London: CABI. 152 pp doi: 10.1079/9781845935719.0000

[4] Bursey CR, Goldberg SR, Grismer LL. 2016. A new species of *Spauligodon* (Nematoda; Oxyuroidea; Pharyngodonide) and other helminths in *Ptychozoon kuhli* (Squamata: Gekkonidae) from East Malaysia. *Acta Parasitologica* 61(2):355–359

[5] Pazoki S, Rahimian H. 2014. New species of *Spauligodon* Skrjabin, Schikhobalova & Lagodovskaja, 1960 and *Thubunea* Seurat, 1914 (Nematoda) from the gastro-intestinal tract of lizards in Iran. *Systematic Parasitology* 89(3):259–270

[6] Casanova JC, Milazzo C, Ribas A, Cagnin M. 2003. *Spauligodon aloisei* n. sp. (Nematoda: Pharyngodonidae) parasite of *Podarcis sicula* (Reptilia: Lacertidae) from Italy. *The Journal of Parasitology* 89(3):577–579

[7] Neves JKS, da Silva GF, Santos AN, Tavares TCS, González CE, et al. 2025. "First of its kind" in Brazilian Amazon: *Spauligodon caxiuana* n. sp. (Nematoda: Pharyngodonidae) parasite of *Thecadactylus rapicauda* (Squamata: Phyllodactylidae), with an updated key to the neotropical and Panamanian species of the genus. *Acta Parasitologica* 70(6):226

[8] Gu XH, Chen HX, Li L. 2026. Morphological and molecular description of *Spauligodon sharpiloi* n.sp. (Nematoda: Oxyurida) from the Mongolian Racerunner *Eremias argus* Peters (Reptilia: Lacertidae). *Parasitology International* 113:103250

[9] Ramallo G, Castillo GN, Acosta JC. 2020. *Parapharyngodon sanjuanensis* (Nematoda, Pharyngodonidae) in the lizard *Phymaturus extrilidus* (Iguania, Liolaemidae) from Puna region, Argentina. *Arxius de Miscel·lània Zoològica* 18:85–88

[10] Ramallo G, Bursey CR, Goldberg SR. 2002. *Spauligodon loboi* n. sp. (Nematoda: Pharyngodonidae) parasite of Liolaemus spp. (Iguania: Liolaemidae) from northwestern Argentina. *The Journal of Parasitology* 88(2):370–374

[11] Abdel-Ghaffar F, Varjabedian KG, Fol M, Talal N, Abdel-Gaber R, et al. 2020. Morphological redescription and phylogenetic assessment of *Spauligodon aspiculus* (Oxyuroidea: Pharyngodonidae) infecting the white-spotted gecko, *Tarentola annularis* (Squamata: Gekkonidae). *Microscopy Research and Technique* 83(8):901–919

[12] Read CP, Amrein YU. 1953. North American nematodes of the genus *Pharyngodon* Diesing (Oxyuridae). *The Journal of Parasitology* 39(4):365–370

[13] Wang T, Yan X, Jiang Z, Xu J, Zhao Y, et al. 2025. New species of *Parapharyngodon* (Nematoda: Pharyngodonidae) parasite of *Laudakia stoliczkana* (Lacertilia: Agamidae) from Turpan-Hami Basin, China. *International Journal for Parasitology: Parasites and Wildlife* 27:101107

[14] Yan XF, Wang T, Zhao YY, Chen ST, Wang YN. 2025. Redescription and revised classification status of *Abbreviata phrynocephali* comb. Nov. (Spirurida: Physalopteridae) from the Yarkand Toad-Headed *Agama Phrynocephalus axillaris* (Lacertilia: Agamidae). *Zootaxa* 5633(2):336–350

[15] Adamson ML. 1981. *Parapharyngodon osteopili* n. sp. (Pharyngodonidae: Oxyuroidea) and a revision of *Parapharyngodon* and *Thelandros*. *Systematic Parasitology* 3:105–117

[16] Banks JC, Paterson AM. 2005. Multi-host parasite species in cophylogenetic studies. *International Journal for Parasitology* 35(7):741–746

[17] Abebe E, Mekete T, Thomas WK. 2011. A critique of current methods in nematode taxonomy. *African Journal of Biotechnology* 10(3):312–323

[18] Mockett S, Bell T, Poulin R, Jorge F. 2017. The diversity and evolution of nematodes (Pharyngodonidae) infecting New Zealand lizards. *Parasitology* 144(5):680–691

[19] González-Rivas CJ, Castillo GN, Acosta JC. 2022. *Skrjabinodon castillensis* n. sp. (Nematoda: Pharyngodonidae) from the *Homonota horrida* and *H. darwinii* (Squamata: Phyllodactylidae) from Argentina and key for the Neotropical species of the genus *Skrjabinodon*. *Annals of Parasitology* 68:483–489

[20] Bursey CR, Goldberg SR. 2005. Two new species of Pharyngodonidae (Nematoda: Oxyuroidea) and other nematodes in *Agama caudospina* (Squamata: Agamidae) from Kenya, Africa. *The Journal of Parasitology* 91(3):591–599

[21] Jorge F, Perera A, Roca V, Carretero MA, Harris DJ, et al. 2014. Evolution of alternative male morphotypes in oxyurid nematodes: a case of convergence? *Journal of Evolutionary Biology* 27(8):1631–1643

[22] Ainsworth R. 1990. Male dimorphism in two new species of nematode (Pharyngodonidae: Oxyurida) from New Zealand lizards. *The Journal of Parasitology* 76(6):812–822

[23] Skrjabin KI, Shikhobalova NP, Lagodovskaya EA. 1960. *Principles of nematology (Osnovy nematodologii)*. Vol. 8. Oxyurata of animals and man. Part 1. Moscow: Nauka. 557 pp (in Russian)

[24] Anderson RC, Chabaud AG, Willmott S. 2009. *Keys to the nematode parasites of vertebrates: archival volume*. London: CABI. doi: 10.1079/9781845935726.0000

[25] Hodda M. 2022. Phylum Nematoda: a classification, catalogue and index of valid Genera, with a census of valid species. *Zootaxa* 5114(1):1–289

[26] Yu X, Xu W, Zhou J, Zhao P, Du M, et al. 2025. 近 30 年吐鲁番盆地坎儿井年径流量变化特征 [Characteristics of change in annual runoff volume of karez in theTurpan Basin in recent 30 years]. *地质科技通报 [Bulletin of Geological Science and Technology]* 44(6):259–269 (in Chinese)

[27] Duan Z. 2018. 吐鲁番沙虎食性的季节变化及其对刺山柑种子扩散综合征的初步研究 *[Seasonal changes in the diet of Teratoscincus roborowskii and preliminary research on the dispersal syndrome to the seed of Capparis spinosa]*. Thesis. Xinjiang Agricultural University, China. (in Chinese) doi: 10.27431/d.cnki.gxnyu.2018.000214

[28] Liu Y, Song Y, Li W, Shi L. 2010. 吐鲁番沙虎头、体大小的两性异形及其食性的季节性变化 [Sexual dimorphism in head and body size of *Teratoscincus roborowskii* and its food habits in different seasons]. *生态学杂志 [Chinese Journal of Ecology]* 29(2):333–338 (in Chinese)

[29] Leng L, Shi L. 2025. How foraging mode sculpts sensory systems: morphological evidence from DiceCT and histology in sympatric lizards. *Ecology and Evolution* 15(8):e72042

[30] Yang Y, Lin Y, Shi L. 2021. The effect of lizards on the dispersal and germination of *Capparis spinosa* (Capparaceae). *PLoS One* 16(2):e0247585

[31] Simmons BI, Sutherland WJ, Dicks LV, Albrecht J, Farwig N, et al. 2018. Moving from frugivory to seed dispersal: incorporating the functional outcomes of interactions in plant–frugivore networks. *Journal of Animal Ecology* 87(4):995–1007

[32] Zwolak R, Bogdziewicz M, Crone EE. 2020. On the need to evaluate costs and benefits of synzoochory for plant populations. *Journal of Ecology* 108(5):1784–1788

[33] Picard M, Papaïx J, Gosselin F, Picot D, Bideau E, et al. 2015. Temporal dynamics of seed excretion by wild ungulates: implications for plant dispersal. *Ecology and Evolution* 5(13):2621–2632

[34] Beveridge I, Hobbs R, Slapeta J. 2015. Parasites. In *Australasian Animal Parasites: Inside and Out*, eds Beveridge I, Emery D. Australia: Australian Society for Parasitology. pp. 25–305

[35] Gardner SL, del Rosario Robles M, Callejón Fernández R, Janovy JJ Jr, Nadler SA, et al. 2024. *Concepts in Animal Parasitology, Part 4: Nemata, Nematomorpha, Acanthocephala, Pentastomida*, eds. Gardner SL, Gardner SA. Lincoln: Zea Books. pp. 532–731 doi: 10.32873/unl.dc.ciap074

[36] Lü L, Zhang SJ, Gu XH, Zhang D, Hugot JP, et al. 2026. Phylogenomics and the evolutionary history of the Oxyurida (pinworms). *Cladistics* 00:Early View

[37] Adamson M. 1994. Evolutionary patterns in life histories of Oxyurida. *International Journal for Parasitology* 24(8):1167–1177

[38] Adamson ML. 1989. Evolutionary biology of the Oxyurida (Nematoda): biofacies of a haplodiploid taxon. *Advances in Parasitology* 28:175–228

[39] Grear DA, Hudson P. 2011. The dynamics of macroparasite host-self-infection: a study of the patterns and processes of pinworm (Oxyuridae) aggregation. *Parasitology* 138(5):619–627

[40] Yan X, Liu M, He S, Tong T, Liu Y, et al. 2021. An epidemiological study of gastrointestinal nematode and *Eimeria coccidia* infections in different populations of Kazakh sheep. *PLoS One* 16(5):e0251307

[41] Floyd RM, Rogers AD, Lambshead PJD, Smith CR. 2005. Nematode-specific PCR primers for the *18S* small subunit rRNA gene. *Molecular Ecology Notes* 5(3):611–612

[42] De Barro PJ, Driver F, Naumann ID, Schmidt S, Clarke GM, et al. 2000. Descriptions of three species of *Eretmocerus haldeman* (Hymenoptera: Aphelinidae) parasitising *Bemisia tabaci* (Gennadius) (Hemiptera: Aleyrodidae) and *Trialeurodes vaporariorum* (Westwood) (Hemiptera: Aleyrodidae) in Australia based on morphological and molecular data. *Australian Journal of Entomology* 39(4):259–269

[43] Zhang D, Gao F, Jakovlić I, Zou H, Zhang J, et al. 2020. PhyloSuite: an integrated and scalable desktop platform for streamlined molecular sequence data management and evolutionary phylogenetics studies. *Molecular Ecology Resources* 20(1):348–355

[44] Holt BG, Lessard JP, Borregaard MK, Fritz SA, Araújo MB, et al. 2013. An update of Wallace's zoogeographic regions of the world. *Science* 339(6115):74–78

[45] Bursey CR, Goldberg SR, Kraus F. 2005. New species of *Spauligodon* (Nematoda: Pharyngodonidae) in *Lepidodactylus novaeguineae* (Sauria: Gekkonidae) from Papua New Guinea. *The Journal of Parasitology* 91(2):324–328

[46] Castillo GN, González-Rivas C, Acosta JC. 2023. *Skrjabinodon castillensis* (Nematode: Pharyngodonidae) parasitizing *Liolaemus gracielae* lizard (Squamata: Iguania: Liolaemidae) from Argentina. *Annals of Parasitology* 69(1):37–41

[47] Jorge F, Perera A, Carretero MA, Harris DJ, Roca V. 2013. Cryptic species unveiled: the case of the nematode *Spauligodon atlanticus*. *Journal of Zoological Systematics and Evolutionary Research* 51(3):187–202

[48] Jorge F, Carretero MA, Perera A, Harris DJ, Roca V. 2012. A new species of *Spauligodon* (Nematoda: Oxyurida: Pharyngodonidae) in geckos from São Nicolau Island (Cape Verde) and its phylogenetic assessment. *The Journal of Parasitology* 98(1):160–166

[49] Ferreira ACS, Vieira FM, Diniz MC, Silva DCN, Ribeiro LB, et al. 2025. First molecular characterisation of a species of *Pharyngodon* Diesing, 1861 (Nematoda: Pharyngodonidae), and description of *Pharyngodon ameivulum* n.sp. in a lizard from Caatinga in Brazil. *Journal of Helminthology* 99:e27

[50] Binh T, Bursey C, Goldberg S. 2007. Two new species of Pharyngodonidae (Nematoda: Oxyuroidea) in *Gekko ulikovskii* from Vietnam. *Acta Parasitologica* 52(4):363–367

[51] Chabaud AG, Brygoo ER. 1962. Nématodes parasites de Caméléons malgaches: Deuxième note. *Annales de Parasitologie Humaine et Comparée* 37(4):569–602 (in French)

[52] Petter AJ. 1966. *Équilibre des espèces dans les populations de nématodes parasites du colon des tortues terrestres [Species balance in populations of parasitic nematodes from the colon of terrestrial tortoises]*. Thesis. University of Paris, France. pp. 1–256 (in French)

[53] Roca V. 2023. Islands, saurians and parasites. *Basic and Applied Herpetology* 37:5–27

[54] Bursey CR, Goldberg SR. 2012. A new species of *Spauligodon* (Nematoda: Oxyuroidea: Pharyngodonidae) in *Gonatodes antillensis* (Squamata: Sphaerodactylidae) from Bonaire, Lesser Antilles. *The Journal of Parasitology* 98(2):344–346

[55] Dornburg A, Lamb AD, Warren D, Watkins-Colwell GJ, Lewbart GA, et al. 2019. Are geckos paratenic hosts for Caribbean island acanthocephalans? Evidence from *Gonatodes antillensis* and a global review of squamate reptiles acting as transport hosts. *Bulletin of the Peabody Museum of Natural History* 60(1):55–79

[56] Bursey CR, Goldberg SR, Telford SR. 2007. New species of *Spauligodon* (Nematoda: Pharyngodonidae) in *Xenosaurus platyceps* (Squamata: Xenosauridae) from Mexico. *Zootaxa* 1501(1):65–68

[57] Cooper WE Jr, Lemos-Espinal JA, Smith GR. 1998. Presence and effect of defensiveness or context on detectability of prey chemical discrimination in the lizard *Xenosaurus platyceps*. *Herpetologica* 54(3):409–413

[58] Ibrahim AA. 2013. Ecology of the rough-tailed Gecko, *Cyrtopodion scabrum* (Squamata: Gekkonidae) in the Suez Canal zone, Egypt. *Journal of Herpetology* 47(1):148–155

[59] Bursey CR, Goldberg SR, Kraus F. 2017. A new species of *Spauligodon* (Nematoda; Oxyuroidea; Pharyngodonidae) and other Nematodes in *Cyrtodactylus epiroticus* (Squamata; Gekkonidae) from Papua, New Guinea. *Acta Parasitologica* 62(4):842–845

[60] Oliver PM, Skipwith P, Lee MS. 2014. Crossing the line: increasing body size in a trans-Wallacean lizard radiation (*Cyrtodactylus*, Gekkota). *Biology Letters* 10(10):20140479

[61] Seurat LG. 1917. Sur les Oxyures des Sauriens du Nord Africain [On the pinworms of North African lizards]. *Archives de Zoologie Expérimentale et Générale [Archives of Experimental and General Zoology]* 56:401–444 (in French)

[62] Bursey CR, Goldberg SR. 1996. *Spauligodon hemidactylus* n. sp. (Nematoda: Pharyngodonidae) from *Hemidactylus frenatus* (Reptilia: Gekkonidae) from Oceania. *The Journal of Parasitology* 82(2):299–301

[63] Díaz Pérez JA, Dávila Suárez JA, Alvarez García DM, Sampedro Marín AC. 2012. Dieta de *Hemidactylus frenatus* (Sauria: Gekkonidae) en un área urbana de la región Caribe Colombiana [Diet of *Hemidactylus frenatus* (Sauria: Gekkonidae) in an urban area of the Colombian Caribbean Region]. *Acta zoológica mexicana [Acta Zoologica Mexicana]* 28:613–616 (in Spanish)

[64] Chitwood BG. 1938. Some nematodes from the caves of Yucatan. *Carnegie Institution of Washington Publication archives N* 491:51–66

[65] Quesnel VC. 2008. Food and feeding behaviour of the nocturnal neotropical gecko *Thecadactylus rapicauda* (Houttuyn) in a dwelling house in Trinidad, West Indies. *Living World, Journal of the Trinidad and Tobago Field Naturalists' Club* 2008:19–27

[66] Spaul EA. 1926. On a new species of the Nematode genus *Pharyngodon*. *Annals and Magazine of Natural History* 17(101):585–591

[67] Hering-Hagenbeck SF, Boomker J. 1998. *Spauligodon timbavatiensis* n. sp. (Nematoda: Pharyngodonidae) from *Pachydactylus turneri* (Sauria: Gekkonidae) in the northern province, South Africa. *The Onderstepoort Journal of Veterinary Research* 65(3):153–158

[68] Molina-Borja M. 2003. Sexual dimorphism of *Gallotia atlantica atlantica* and *Gallotia atlantica mahoratae* (Lacertidae) from the Eastern Canary Islands. *Journal of Herpetology* 37(4):769–772

[69] Piazzon M, Larrinaga AR, Rodríguez-Pérez J, Latorre L, Navarro L, et al. 2012. Seed dispersal by lizards on a continental-shelf island: predicting interspecific variation in seed rain based on plant distribution and lizard movement patterns. *Journal of Biogeography* 39(11):1984–1995

[70] Escorcia-Ignacio R, Monks S, Pulido-Flores G. 2008. A new species of *Spauligodon* (Nematoda: Pharyngodonidae) in *Sceloporus* (Squamata: Phrynosomatidae) from the reserve of the biosphere Barranca de Metztitlán, Hidalgo, Mexico. *Revista Mexicana de Biodiversidad* 79:129–133

[71] García-Rosales A, Ramírez-Bautista A, Stephenson BP. 2019. Comparative morphology and trophic ecology in a population of the polymorphic lizard *Sceloporus minor* (Squamata: Phrynosomatidae) from central Mexico. *PeerJ* 7:e8099

[72] Clayton DH, Al-Tamimi S, Johnson KP. 2003. The ecological basis of coevolutionary history. In T*angled Trees: Phylogeny, Cospeciation, and Coevolution*, ed. Page RDM. Chicago: University of Chicago Press. pp. 310–341

[73] Martin JE, Roca V. 2004. Helminth infracommunities of *Gallotia caesaris caesaris* and *Gallotia caesaris gomerae* (Sauria: Lacertidae) from the Canary Islands (Eastern Atlantic). *The Journal of Parasitology* 90(2):266–270

[74] Page RDM. 2003. *Tangled trees: Phylogeny, cospeciation, and coevolution*. Chicago: University of Chicago Press. 350 pp